

NONLINEAR GEOMETRIC OPTICS BASED MULTISCALE STOCHASTIC GALERKIN METHODS FOR HIGHLY OSCILLATORY TRANSPORT EQUATIONS WITH RANDOM INPUTS

NICOLAS CROUSEILLES¹, SHI JIN^{2,*}, MOHAMMED LEMOU³ AND LIU LIU⁴

Abstract. We develop generalized polynomial chaos (gPC) based stochastic Galerkin (SG) methods for a class of highly oscillatory transport equations that arise in semiclassical modeling of non-adiabatic quantum dynamics. These models contain uncertainties, particularly in coefficients that correspond to the potentials of the molecular system. We first focus on a highly oscillatory scalar model with random uncertainty. Our method is built upon the nonlinear geometrical optics (NGO) based method, developed in Crouseilles *et al.* [*Math. Models Methods Appl. Sci.* **23** (2017) 2031–2070] for numerical approximations of deterministic equations, which can obtain accurate pointwise solution even without numerically resolving spatially and temporally the oscillations. With the random uncertainty, we show that such a method has oscillatory higher order derivatives in the random space, thus requires a frequency dependent discretization in the random space. We modify this method by introducing a new “time” variable based on the phase, which is shown to be non-oscillatory in the random space, based on which we develop a gPC-SG method that can capture oscillations with the frequency-independent time step, mesh size as well as the degree of polynomial chaos. A similar approach is then extended to a semiclassical surface hopping model system with a similar numerical conclusion. Various numerical examples attest that these methods indeed capture accurately the solution statistics *pointwisely* even though none of the numerical parameters resolve the high frequencies of the solution.

Mathematics Subject Classification. 35Q40, 35L03, 74Q10, 65M12.

Received June 27, 2018. Accepted December 19, 2019.

1. INTRODUCTION

Computational high frequency waves is challenging since one needs to numerically resolve the small wave length which is often prohibitively expensive [9]. Recently, a nonlinear geometric optics (NGO) based numerical

Keywords and phrases. Highly oscillatory PDEs, nonlinear geometric optics, asymptotic preserving, uncertainty quantification, generalized polynomial chaos, stochastic Galerkin method, surface hopping.

¹ Univ Rennes, Inria Rennes & Institut de Recherche Mathématiques de Rennes, CNRS UMR 6625 Rennes & ENS Rennes, Rennes, France.

² School of Mathematical Sciences, Institute of Natural Sciences, MOE-LSC and SHL-MAC, Shanghai Jiao Tong University, Shanghai, P.R. China.

³ Univ Rennes, CNRS & Institut de Recherche Mathématiques de Rennes, CNRS UMR 6625 & Inria Rennes & ENS Rennes, Rennes, France.

⁴ Department of Mathematics, The Chinese University of Hong Kong, Shatin, N.T., Hong Kong SAR.

*Corresponding author: shijin-m@sjtu.edu.cn, jin@math.wisc.edu

method was introduced in [8] for a class of highly oscillatory transport equations which allows the use of mesh size and time step *independent* of the wave length. The transport equations that were solved by this method are deterministic and are relevant to semiclassical approximations to quantum dynamics with band-crossings [3, 4, 15, 16], a general non-adiabatic quantum mechanics phenomenon that can be found in a variety of important physics and chemistry problems, such as chemical reaction [21, 22], Bose–Einstein condensation [25], and graphene [2, 10].

These semiclassical models were approximations of the nucleonic Schrödinger equations, in which the potential matrices were obtained by solving the electronic eigenvalue problems, based on the Born–Oppenheimer approximation [1]. The computation of electronic eigenvalue problems is a grand challenge in quantum dynamics, and many approximation tools, for example the density functional theory (DFT) [17], were developed. In the DFT theory, the dispersion was treated incompletely thus will inevitably affect the accuracy of DFT when the dispersion is strong [23, 24]. Due to these inaccuracies, the potential matrices, or the band gaps, will contain *uncertainties*. Uncertainties could arise in the boundary or initial data, and forcing terms, due to inaccurate approximations or experiment measurements. Thus the study of uncertainty quantification is of great importance in quantum dynamics and chemical reacting systems [18, 19]. In this paper, we are interested in the random uncertainty of the potential energy surface, and the goal is to develop efficient computational methods to compute the propagation of the uncertainty. As is typical in uncertainty quantification, we model the uncertainty by random inputs [11, 26]. For such uncertain problems, the so-called gPC-SG methods (combination of generalized polynomial chaos (gPC) approximation with stochastic Galerkin (SG) projections) are known to be efficient for a wide range of partial differential equations with random uncertainties (see *e.g.* [11, 13, 14, 26, 28]). However, direct application of such methods to highly-oscillatory problems with uncertainty becomes computationally expensive if one wants to correctly capture the effect of these oscillations, since one needs to resolve numerically the oscillations. In this paper, we are interested in extending the nonlinear geometric optics (NGO)-based method, which was developed in [8] for a class of highly-oscillatory deterministic problems, to highly-oscillatory problems with uncertainty, in the framework of gPC-SG methods. In particular, we will develop here gPC-SG methods that not only allow the mesh size and time step, *but also the order of the gPC approximation, to be independent of the small wave length.*

We develop the gPC-SG methods for two model equations: a scalar model transport equation and a semiclassical surface hopping model developed in [4]. Both models were studied in [8] in the deterministic case. Here we assume random coefficients in these models that correspond to the band-gap in the non-adiabatic quantum dynamics, and the band gap could become small to model the so-called avoided crossing in which the quantum transition between bands is significant. With the random uncertainty, we first show that such a method is oscillatory for higher order derivatives in the random space, thus requires a frequency dependent discretization in the random space, which becomes prohibitively expensive to compute. We then modify this method by introducing a new “time” variable based on the phase, which is shown to be non-oscillatory in the random space, based on which we develop a gPC-SG method that can capture the pointwise solution with *frequency-independent* time step, mesh size as well as the degree of polynomial chaos. This method is then extended to the semiclassical model of surface hopping with random band gap, with the same numerical property.

The paper is organized as follows. In Section 2, using a scalar equation with uncertain random coefficient, we develop the gPC-SG method by either solving the equation directly, or using the NGO approach. We prove that in both cases the method needs to use wave frequency dependent gPC order (although for the latter method such a dependence is one order milder). Based on a theoretical result of [8], we introduce a new time variable using the phase, which will be shown to be non-oscillatory also in the random space, allowing us to develop a new NGO-based method which are capable of obtaining accurate pointwise solution without resolving the oscillations by any of the numerical parameters. Numerical examples will verify the theoretical property as well as the aforementioned numerical properties. This method is then extended to a semiclassical surface hopping model in Section 3, with the same numerical properties which are demonstrated numerically in Section 4. We conclude the paper in Section 5.

2. THE ONE DIMENSIONAL SCALAR EQUATION WITH RANDOM INPUTS

In this section we consider a one dimensional problem with random inputs. Here the unknown is $u(t, x, \mathbf{z}) \in \mathbb{C}$, where $x \in \Omega \subset \mathbb{R}$, $t \geq 0$, and $\mathbf{z} \in I_{\mathbf{z}} \subset \mathbb{R}^n$, $n \geq 1$, is the random variable with a prescribed probability density function $\pi(\mathbf{z})$. We consider the following scalar model for u :

$$\partial_t u + c(x)\partial_x u + r(u) = \frac{ia(x, \mathbf{z})}{\varepsilon} u, \quad u(0, x, \mathbf{z}) = u_{in}(x, \mathbf{z}), \tag{2.1}$$

where $a(x, \mathbf{z})$, $c(x)$, $r(u)$ and $u_{in}(x, \mathbf{z})$ are all given functions, with $a \geq 0$. We assume that Ω is a bounded interval and that periodic boundary conditions are considered for the space variable x . Even if it induces technical difficulties, the source term a can also depend on the time variable. Moreover, we assume here that the initial condition u_{in} is non-oscillatory.

2.1. A gPC-SG framework

We briefly describe the SG method. See for examples [14, 26, 28]. Let \mathbb{P}_P^n be the space of the n -variate polynomials of degree less than or equal to $P \geq 1$, and recall that

$$\dim(\mathbb{P}_P^n) = \text{card}\{\mathbf{k} \in \mathbb{N}^n, |\mathbf{k}| \leq P\} = \binom{n+P}{P} := K, \tag{2.2}$$

where we have denoted $\mathbf{k} = (k_1, \dots, k_n)$ and $|\mathbf{k}| = k_1 + \dots + k_n$. We consider the following inner product

$$\langle f, g \rangle_{\pi} = \int_{I_{\mathbf{z}}} f(\mathbf{z})g(\mathbf{z})\pi(\mathbf{z}) \, d\mathbf{z}, \quad \forall f, g \in L^2(\pi(\mathbf{z}) \, d\mathbf{z}),$$

where $L^2(\pi(\mathbf{z}) \, d\mathbf{z})$ is the usual weighted Lebesgue space, and its associated norm is

$$\|f\|_{L^2(\pi(\mathbf{z}) \, d\mathbf{z})}^2 = \int_{I_{\mathbf{z}}} |f(\mathbf{z})|^2 \pi(\mathbf{z}) \, d\mathbf{z}.$$

Consider a corresponding orthonormal basis $\{\psi_{\mathbf{k}}(\mathbf{z})\}_{\mathbf{k} \in \mathbb{N}^n, |\mathbf{k}| \leq P}$ of the space \mathbb{P}_P^n , where the degree of $\psi_{\mathbf{k}}$ is $\text{deg}(\psi_{\mathbf{k}}) = |\mathbf{k}|$. In particular

$$\langle \psi_{\mathbf{k}}, \psi_{\mathbf{l}} \rangle_{\pi} = \int_{I_{\mathbf{z}}} \psi_{\mathbf{k}}(\mathbf{z})\psi_{\mathbf{l}}(\mathbf{z})\pi(\mathbf{z}) \, d\mathbf{z} = \delta_{\mathbf{k}\mathbf{l}}, \quad |\mathbf{k}|, |\mathbf{l}| \leq P,$$

where $\delta_{\mathbf{k}\mathbf{l}}$ is the Kronecker symbol. The commonly used pairs of $\{\psi_{\mathbf{k}}(\mathbf{z})\}$ and $\pi(\mathbf{z})$ include Hermite–Gaussian, Legendre-uniform, Laguerre–Gamma, etc. Since the family $\{\psi_{\mathbf{k}}(\mathbf{z})\}_{|\mathbf{k}| \leq P}$ has K elements we introduce its renumbering family $(\tilde{\psi}_1, \tilde{\psi}_2, \dots, \tilde{\psi}_K)$, that is

$$\{\psi_{\mathbf{k}}(\mathbf{z})\}_{\mathbf{k} \in \mathbb{N}^n, |\mathbf{k}| \leq P} = (\tilde{\psi}_1, \tilde{\psi}_2, \dots, \tilde{\psi}_K), \quad \text{deg}(\tilde{\psi}_j) \leq \text{deg}(\tilde{\psi}_{j+1}).$$

The SG method consists in seeking the solution to (2.1) as a projection onto the space \mathbb{P}_P^n , that is

$$u(t, x, \mathbf{z}) \approx \sum_{|\mathbf{k}| \leq P} u_{\mathbf{k}}(t, x)\psi_{\mathbf{k}}(\mathbf{z}) = \sum_{j=1}^K \tilde{u}_j(t, x)\tilde{\psi}_j(\mathbf{z}), \tag{2.3}$$

with

$$u_{\mathbf{k}} = \langle u, \psi_{\mathbf{k}} \rangle_{\pi}, \quad \tilde{u}_j = \langle u, \tilde{\psi}_j \rangle_{\pi}, \quad |\mathbf{k}| \leq P, \quad j = 1, 2, \dots, K.$$

From this approximation one can easily compute statistical moments, such as the mean and standard deviation, as

$$\mathbb{E}(u) \approx u_{(0, \dots, 0)} = \tilde{u}_1, \quad \text{SD}(u) \approx \left(\sum_{1 \leq |\mathbf{k}| \leq P} |u_{\mathbf{k}}|^2 \right)^{1/2} = \left(\sum_{j=2}^K |\tilde{u}_j|^2 \right)^{1/2}. \tag{2.4}$$

2.2. The direct gPC-SG method

We first introduce the gPC-SG method for the direct method (hereafter called gPC-SG-D) – solving (2.1) directly. For simplicity of illustration, assume $c(x)$ does not depend on \mathbf{z} . The case when c depends on \mathbf{z} can be easily incorporated into the gPC-SG framework [12]. The gPC-SG solution for u is computed through the projection formula (2.3) as follows.

Denote the gPC coefficients

$$\vec{u}(t, x) = (\tilde{u}_1(t, x), \dots, \tilde{u}_K(t, x))^T.$$

Inserting the approximated solution (2.3) to (2.1) and conducting the standard Galerkin projection, one gets

$$\partial_t \vec{u} + c(x)\partial_x \vec{u} + \vec{\gamma}(u) = \frac{i}{\varepsilon} A(x) \vec{u}, \quad \vec{u}(0, x) = \int_{I_{\mathbf{z}}} u_{in}(x, \mathbf{z}) \tilde{\psi}(\mathbf{z}) \pi(\mathbf{z}) \, d\mathbf{z}, \tag{2.5}$$

with

$$\tilde{\psi}(\mathbf{z}) = (\tilde{\psi}_1(z), \tilde{\psi}_2(z), \dots, \tilde{\psi}_K(z))^T, \quad u(t, x, \mathbf{z}) = \sum_{j=1}^K \tilde{u}_j(t, x) \tilde{\psi}_j(\mathbf{z}). \tag{2.6}$$

The j th component of the vector $\vec{\gamma} = (\tilde{\gamma}_1, \tilde{\gamma}_2, \dots, \tilde{\gamma}_K)$ is given by

$$\tilde{\gamma}_j(u) = \int_{I_{\mathbf{z}}} r(u) \tilde{\psi}_j(\mathbf{z}) \pi(\mathbf{z}) \, d\mathbf{z}, \quad \text{for } j = 1, \dots, K, \tag{2.7}$$

and the symmetric, non-negative definite matrix $A \in \mathbb{R}_{K \times K}$ (recall that $a \geq 0$) is defined by

$$A_{s,j}(x) = \int_{I_{\mathbf{z}}} a(x, \mathbf{z}) \tilde{\psi}_s(\mathbf{z}) \tilde{\psi}_j(\mathbf{z}) \pi(\mathbf{z}) \, d\mathbf{z}, \quad \text{for } s, j = 1, \dots, K. \tag{2.8}$$

To solve numerically (2.5), we use a simple time splitting. To this aim, we fix a time step $\Delta t > 0$ and set $t_n = n\Delta t$ for $n \in \mathbb{N}$. As usual, we denote by $\vec{u}^n(x) = (\tilde{u}_1^n(x), \tilde{u}_2^n(x), \dots, \tilde{u}_K^n(x))$ an approximation of $\vec{u}(t_n, x)$. We split system (2.5) in three parts which can be solved as follows.

– **Oscillatory part**

The oscillatory part

$$\partial_t \vec{u} = \frac{i}{\varepsilon} A(x) \vec{u},$$

is solved exactly in time, for each x , to get

$$\vec{u}^{n+1}(x) = \exp\left(\frac{i}{\varepsilon} A(x) \Delta t\right) \vec{u}^n(x).$$

– **Nonlinear part**

To solve the nonlinear part

$$\partial_t \vec{u} + \vec{\gamma}(u) = 0,$$

we choose to use the forward Euler method, that is

$$\vec{u}^{n+1} = \vec{u}^n - \Delta t \vec{\gamma}(u^n). \tag{2.9}$$

To compute $\vec{\gamma}(u^n)$, we first compute $u^n(x, \mathbf{z}) = \sum_{s=1}^K \tilde{u}_s^n(x) \tilde{\psi}_s(\mathbf{z})$ using the Gauss-quadrature rule (where the quadrature points are chosen as the roots of the orthogonal polynomials determined by the distribution π of the random variables, see [28]) to get $\vec{\gamma}(u)$ given by (2.7) as follows. Define the Gauss-quadrature points as $z^{(l)}$ and

the corresponding weights ω_l , $l = 1, \dots, N_g$. The value of $r(u)$ evaluated at x , t and at the Gauss-quadrature point $z^{(l)}$ is given by $r(u(z^{(l)})) = r\left(\sum_{j=1}^K \tilde{u}_j(t, x) \tilde{\psi}_j(z^{(l)})\right)$. By (2.7), one has

$$\tilde{\gamma}_j(u) = \sum_{l=1}^{N_g} r(u(z^{(l)})) \tilde{\psi}_j(z^{(l)}) \omega_l,$$

which is used in (2.9) to get \vec{u}^{n+1} .

– **Transport part**

To solve the transport part

$$\partial_t \vec{u} + c(x) \partial_x \vec{u} = 0,$$

we use a pseudo-spectral method in space and a three-stage Runge–Kutta method in time which was introduced in [6]. Denote $\mathcal{T}(u^n) = -c(x) \mathcal{F}^{-1}(i\xi \mathcal{F}(u^n))$, where \mathcal{F} and \mathcal{F}^{-1} are the (discrete) Fourier and inverse Fourier Transforms respectively, and ξ is the Fourier space variable. Then

$$\begin{aligned} \vec{u}^{n,(1)} &= \vec{u}^n + \frac{1}{2} \Delta t \mathcal{T}(\vec{u}^n), \\ \vec{u}^{n,(2)} &= \vec{u}^n + \frac{1}{2} \Delta t \mathcal{T}(\vec{u}^{n,(1)}), \\ \vec{u}^{n+1} &= \vec{u}^n + \Delta t \mathcal{T}(\vec{u}^{n,(2)}). \end{aligned} \tag{2.10}$$

Notice that the spectral approximation is central type finite difference approximation with purely imaginary spectrum, thus one needs to use ODE solvers that have a stability region that contains part of the purely imaginary axis [6]. The scheme (2.10) is such an ODE solver where the stability region takes the largest part of the imaginary axis among three-stage ODE solvers, and is of second order accuracy in time.

2.3. The NGO-based gPC-SG method

We first review the NGO based method introduced in [8] for the deterministic one-dimensional scalar equation,

$$\partial_t u + c(x) \partial_x u + r(u) = \frac{ia(x)}{\varepsilon} u, \quad u(0, x) = u_{in}(x), \tag{2.11}$$

where the functions u_{in} , a , c and r are given and $a(x) \geq 0$. Periodic boundary conditions in space are considered. For the sake of simplicity, we assume that the initial data u_{in} does not depend on ε , namely, it is non-oscillatory.

We focus on the case when r is nonlinear. We recall how *nonlinear geometric optics* (NGO) is utilized to solve problem (2.11) in [8]. Introduce a profile function $U(t, x, \tau)$ which depends on the 2π -periodic variable τ , and a phase $S(t, x)$ such that

$$U(t, x, S(t, x)/\varepsilon) = u(t, x), \tag{2.12}$$

with u solving (2.11). Inserting this ansatz into (2.11) gives

$$\partial_t U + c(x) \partial_x U + \frac{1}{\varepsilon} [\partial_t S + c(x) \partial_x S] \partial_\tau U + r(U) = \frac{ia(x)}{\varepsilon} U.$$

Due to the periodicity constraint on U , the following equation on the phase S should be imposed (see [8] for details),

$$\partial_t S + c(x) \partial_x S = a(x), \quad S(0, x) = 0, \tag{2.13}$$

then the equation for U is given by

$$\partial_t U + c(x) \partial_x U + r(U) = -\frac{a(x)}{\varepsilon} (\partial_\tau U - iU), \quad U(0, x, 0) = u_{in}(x). \tag{2.14}$$

For convenience, we write (2.14) in terms of $V = e^{-i\tau}U$ and get

$$\partial_t V + c(x)\partial_x V + e^{-i\tau}r(e^{i\tau}V) = -\frac{a(x)}{\varepsilon}\partial_\tau V, \quad V(0, x, 0) = u_{in}(x). \tag{2.15}$$

One needs initial data $V(0, x, \tau)$ for all τ to solve equation (2.15). The only requirement we have to ensure is $V(0, x, 0) = u_{in}(x)$. One critical idea is to use initial data for V so that the solution to (2.15) remains bounded uniformly in ε up to certain order of derivatives.

Introduce the operators \mathcal{L} and Π ,

$$\mathcal{L}g = \partial_\tau g, \quad \Pi g = \frac{1}{2\pi} \int_0^{2\pi} g(\tau) d\tau,$$

and

$$\mathcal{L}^{-1}g = (\mathcal{I} - \Pi) \int_0^\tau g(\sigma) d\sigma = \int_0^\tau g(\sigma) d\sigma + \frac{1}{2\pi} \int_0^{2\pi} \sigma g(\sigma) d\sigma.$$

Following the work of [5, 7, 8], a Chapman–Enskog expansion is used to give a suitable initial condition given by

$$V(0, x, \tau) = u_{in}(x) + \frac{\varepsilon}{a(x)} [\mathcal{G}(0, u_{in}) - \mathcal{G}(\tau, u_{in})], \tag{2.16}$$

$$\text{with } \mathcal{G}(\tau, u_{in}) = \mathcal{L}^{-1}(\mathcal{I} - \Pi) [e^{-i\tau}r(e^{i\tau}u_{in})]. \tag{2.17}$$

It was proved in [8] that the solution V to (2.15) and (2.16) has bounded (*uniformly in ε*) derivatives in both x and t up to second order. Thus it allows the construction of a scheme with a uniform accuracy with respect to ε . We recall in the sequel the scheme introduced in [8].

Consider a uniform partition in time $t_n = n\Delta t$ ($\Delta t > 0$ the time step) of a time interval $[0, T]$, $n = 0, 1, \dots, N$, $N\Delta t = t_N$ and in space $x_j = j\Delta x$, $j = 0, 1, \dots, N_x$, $\Delta x = 1/N_x$ of the spatial interval $[0, 1]$. A uniform mesh is assumed in the direction $\tau \in \mathbb{T} = [0, 2\pi]$, $\tau_l = l\Delta\tau$, $l = 0, \dots, N_\tau$, $\Delta\tau = 2\pi/N_\tau$. Denote by $V_j^n(\tau) \approx V(t_n, x_j, \tau)$ and $S_j^n \approx S(t_n, x_j)$ the discrete unknowns at time t_n , evaluated at x_j .

To solve the equation (2.13) for S , the pseudo-spectral method in space and 4th order Runge–Kutta method in time are used. In other words, the following ODE system on $S_j(t) \approx S(t, j\Delta x)$:

$$\partial_t S_j + c(x_j)\mathcal{F}^{-1}(i\xi\mathcal{F}(S^n))_j = a(x_j), \quad S_j(0) = 0, \tag{2.18}$$

is solved by the 4th order Runge–Kutta method. To recover the original solution u at the final time t_N , we use (2.12) at $t = t_N$ and $x = x_j$. Since S_j^N/ε does not necessarily coincide with a grid point τ_l at the final time $t_N = N\Delta t$, thus one can perform a trigonometric interpolation

$$u(t_N, x_j) \approx V_j^N(\tau = S_j^N/\varepsilon). \tag{2.19}$$

Note that a high order method is required here to solve S since we need to construct the quantity $S(t, x)/\varepsilon$, and the error of S is divided by ε . Then, denoting by p the order of the method ($p = 4$ for the method proposed above), we then require $\Delta t = \mathcal{O}(\varepsilon^{1/p})$ to ensure uniform accuracy for the unknown u . Note that the phase function is smooth since (2.13) does not contain any stiff term and can then be solved independently from the equation on V .

To solve (2.15) for V , we start with V_j^0 given by (2.16) at $x = x_j$. Then, the scheme for V reads (assume $c(x) > 0$)

$$\frac{V_j^{n+1} - V_j^n}{\Delta t} + c(x_j)\frac{V_j^n - V_{j-1}^n}{\Delta x} + e^{-i\tau}r(e^{i\tau}V_j^n) = -\frac{a(x_j)}{\varepsilon}\partial_\tau V_j^{n+1}. \tag{2.20}$$

Here the right hand side is discretized implicitly due to its numerical stiffness and the τ variable is discretized using the Fourier transform.

2.3.1. The gPC-SG-N1 method

Our aim now is to extend the NGO method presented in the previous section to solve a highly oscillatory problem with uncertainty, namely (2.1). By [8], and similarly to (2.13) and (2.15), the NGO-based method solves S from

$$\partial_t S + c(x)\partial_x S = a(x, \mathbf{z}), \quad S(0, x, \mathbf{z}) = 0, \tag{2.21}$$

and solves V from

$$\partial_t V + c(x)\partial_x V + e^{-i\tau} r(e^{i\tau} V) = -\frac{a(x, \mathbf{z})}{\varepsilon} \partial_\tau V, \tag{2.22}$$

with initial data

$$V(0, x, \tau, \mathbf{z}) = u_{in}(x, \mathbf{z}) + \frac{\varepsilon}{a(x, \mathbf{z})} [\mathcal{G}(0, u_{in}, \mathbf{z}) - \mathcal{G}(\tau, u_{in}, \mathbf{z})] \tag{2.23}$$

$$\text{with } \mathcal{G}(\tau, u_{in}, \mathbf{z}) = \mathcal{L}^{-1}(\mathcal{I} - \Pi) [e^{-i\tau} r(e^{i\tau} u_{in})], \tag{2.24}$$

where $u_{in}(x, \mathbf{z})$ and $a(x, \mathbf{z})$ now depend on \mathbf{z} . Below we detail the gPC approach for this system.

The gPC formulation for S

One inserts the gPC-SG ansatz

$$S(t, x, \mathbf{z}) \approx \sum_{|\mathbf{k}| \leq P} S_{\mathbf{k}}(t, x) \psi_{\mathbf{k}}(\mathbf{z}) = \sum_{j=1}^K \tilde{S}_j(t, x) \tilde{\psi}_j(\mathbf{z})$$

into (2.21) and conducts the Galerkin projection, to get

$$\partial_t \vec{S} + c(x)\partial_x \vec{S} = \vec{\mathcal{R}}(x), \quad \vec{S}(0, x) = 0, \tag{2.25}$$

where the gPC coefficients \vec{S} is defined by

$$\vec{S}(t, x) = \left(\tilde{S}_1(t, x), \dots, \tilde{S}_K(t, x) \right)^T,$$

and

$$\vec{\mathcal{R}}(x) = \int_{I_{\mathbf{z}}} a(x, \mathbf{z}) \tilde{\psi}(\mathbf{z}) \pi(\mathbf{z}) d\mathbf{z}. \tag{2.26}$$

We recall the notation: $\tilde{\psi} = (\tilde{\psi}_1, \tilde{\psi}_2, \dots, \tilde{\psi}_K)$.

The gPC formulation for V

We insert the gPC-SG ansatz

$$V(t, x, \tau, \mathbf{z}) \approx \sum_{|\mathbf{k}| \leq P} V_{\mathbf{k}}(t, x, \tau) \psi_{\mathbf{k}}(\mathbf{z}) = \sum_{j=1}^K \tilde{V}_j(t, x, \tau) \tilde{\psi}_j(\mathbf{z})$$

into (2.22) and conduct the Galerkin projection to get

$$\partial_t \vec{V} + c(x)\partial_x \vec{V} + e^{-i\tau} \vec{\gamma}(e^{i\tau} V) = -\frac{1}{\varepsilon} A(x) \partial_\tau \vec{V}, \tag{2.27}$$

where A is the matrix given by (2.8) and

$$\vec{V}(t, x, \tau) = \left(\tilde{V}_1(t, x, \tau), \dots, \tilde{V}_K(t, x, \tau) \right)^T.$$

The j th component $\tilde{\gamma}_j$ of the vector $\vec{\gamma}$ is

$$\tilde{\gamma}_j(e^{i\tau}V) = \int_{I_{\mathbf{z}}} r(e^{i\tau}V)\tilde{\psi}_j(\mathbf{z})\pi(\mathbf{z})\,d\mathbf{z}, \quad \text{for } j = 1, \dots, K, \quad (2.28)$$

which is computed by the Gauss-quadrature formula.

The initial data

Here we consider that $a(x, \mathbf{z})$ depends on the random variable \mathbf{z} . The gPC approximation of the initial condition (2.23) becomes

$$\vec{V}(0, x, \tau) = \mathbf{T} + \varepsilon \mathbf{Y}, \quad (2.29)$$

where the vectors $\mathbf{T} \in \mathbb{R}^K$ and $\mathbf{Y} \in \mathbb{R}^K$ are given by

$$\begin{aligned} \mathbf{T}(x) &= \int_{I_{\mathbf{z}}} u_{in}(x, \mathbf{z})\tilde{\psi}(\mathbf{z})\pi(\mathbf{z})\,d\mathbf{z}, \\ \mathbf{Y}(x, \tau) &= \int_{I_{\mathbf{z}}} \frac{1}{a(x, \mathbf{z})} [\mathcal{G}(0, u_{in}, \mathbf{z}) - \mathcal{G}(\tau, u_{in}, \mathbf{z})]\tilde{\psi}(\mathbf{z})\pi(\mathbf{z})\,d\mathbf{z}, \end{aligned}$$

with $\tilde{\psi}(\mathbf{z})$ given in (2.6).

2.3.2. The fully discrete gPC-SG-N1 method

Now we discretize (2.21) and (2.22) in time as in the deterministic case. The phase vector \vec{S} is obtained by applying a pseudo-spectral method in space, which leads to the following semi-discretized equation

$$\partial_t \vec{S}_j + c(x_j)\mathcal{F}^{-1}\left(i\xi\mathcal{F}(\vec{S})\right)_j = \vec{\mathcal{R}}(x_j), \quad \vec{S}_j(0) = 0, \quad \forall j = 0, \dots, N_x, \quad (2.30)$$

where $\vec{\mathcal{R}}(x)$ is given by (2.26). Here, $\vec{S}_j(t)$ is an approximation of $\vec{S}(t, x_j)$ and the same notation is used for other quantities. Then a 4th order Runge–Kutta method is applied to march in time.

To solve the equation on \vec{V} , knowing \vec{S} , we start by the initial value \vec{V}_j^0 given by (2.29) at grid points $x = x_j$. Then the system is advanced in time by a simple time-splitting algorithm as explained for the deterministic case in Section 2.2. The nonlinear part (the $\vec{\gamma}$ term) and the transport part are treated in the same way as in Section 2.2. For the oscillatory part, we use the backward Euler method in time:

$$\frac{\vec{V}_j^{n+1} - \vec{V}_j^n}{\Delta t} = -\frac{1}{\varepsilon}A(x_j)\partial_\tau \vec{V}_j^{n+1}, \quad (2.31)$$

where $\vec{V}_j^n(\tau)$ is an approximation of $\vec{V}(n\Delta t, x_j, \tau)$ and A is given by (2.8). Let $\vec{V}_j^n(\zeta)$ be the Fourier transform of $\vec{V}_j^n(\tau)$ in the periodic variable τ , where ζ is the Fourier variable. The spectral method is used to discretize the τ -derivative, then (2.31) becomes (removing the dependency in ζ)

$$\vec{V}_j^{n+1} = \left[I + i\zeta \frac{\Delta t}{\varepsilon} A(x_j) \right]^{-1} \vec{V}_j^n. \quad (2.32)$$

The updated values \vec{V}_j^{n+1} are then obtained by the inverse Fourier transform. Note that since A is non-negative definite, all its eigenvalues are real and non-negative. Thus the matrix $I + i\zeta \frac{\Delta t}{\varepsilon} A$ has non-zero eigenvalues, thus is invertible. In the sequel, we refer this method as the gPC-SG-N1 method.

2.4. The relation between the gPC order K and ε

The main advantage of the NGO-based method over the direct method is that the former allows one to use Δt and Δx independent of ε , thus when ε is small, one can still use relatively larger Δt and Δx to get accurate solution at the mesh points. In this section, we prove that this remarkable property is not true for the random approximation, namely *one can not use the gPC order K independent of ε* either for the gPC-SG-D or gPC-SG-N1.

– The gPC-SG-D

To show the gPC-SG-D method does not satisfy the uniform accuracy property, we consider the simple case where the functions c and a are independent of x , and where $\mathbf{z} \in \mathbb{R}$:

$$\partial_t u + c \partial_x u = \frac{ia(\mathbf{z})}{\varepsilon} u.$$

By the method of characteristics, the analytic solution is given by

$$u(t, x, \mathbf{z}) = e^{\frac{ia(\mathbf{z})}{\varepsilon} t} u_{in}(x - ct, \mathbf{z}),$$

where u_{in} is the initial data. Taking the q th order derivative in \mathbf{z} , one sees that $\partial_{\mathbf{z}}^q u = O(1/\varepsilon^q)$.

Assume $u_{in} \in H_{\mathbf{z}}^q(\pi(\mathbf{z}) \, d\mathbf{z})$, where $H_{\mathbf{z}}^q$ is the Sobolev space in \mathbf{z} defined as

$$\|u\|_{H_{\mathbf{z}}^q} = \left(\sum_{l=0}^q \|\partial_{\mathbf{z}}^l u\|_{L^2(\pi(\mathbf{z}) \, d\mathbf{z})} \right)^{\frac{1}{2}}.$$

By the standard approximation theory of orthogonal polynomials (see *e.g.* [20]), one has

$$\left\| u - \sum_{j=1}^K \tilde{u}_j \tilde{\psi}_j \right\|_{L^2(\pi(\mathbf{z}) \, d\mathbf{z})} \leq \frac{C}{\varepsilon^q K^q},$$

where C is a constant depending on t , the derivatives of $a(\mathbf{z})$ and u_{in} with respect to \mathbf{z} . This shows that one needs to take K inversely proportional to ε in order to ensure an accurate approximation in \mathbf{z} .

– The gPC-SG-N1

We consider the gPC-SG-N1 method and show that the degree of the polynomial approximation needs to be chosen dependent on ε to ensure a spectral accuracy. To this aim, we analyze the projection error on the function V , solution to (2.22),

$$\partial_t V + c(x) \partial_x V + e^{-i\tau} r(e^{i\tau} V) = -\frac{a(x, \mathbf{z})}{\varepsilon} \partial_{\tau} V. \tag{2.33}$$

From (2.33), clearly, the l th derivative in z of V satisfies basically the *same* equation as the l th derivative in x of V (except one involves the derivatives of a in z while the other involves the derivatives of a in x). Therefore, as long as a and u_{in} have the same regularity in x and z , V will have the *same* regularity in x and z . Since with the choice of initial data (2.23), we only guarantee bounded (in terms of ε) x derivatives of V up to the second order, therefore, we only have up to second bounded derivatives in z for V . This is clearly not enough for SG methods (nor for the stochastic collocation method, to be introduced later) which can achieve high order-up to spectral-accuracy if there is sufficient regularity in the solution.

2.5. A new NGO-based gPC-SG method (gPC-SG-N2)

In the following, we show how to construct a numerical method for which the derivatives of V with respect to \mathbf{z} and x are bounded uniformly in ε at *any* order. To this aim, let us consider the following change of function

$$V(t, x, \mathbf{z}, \tau) = W(S(t, x, \mathbf{z}), x, \mathbf{z}, \tau), \tag{2.34}$$

where S solves (2.21). Then, W is the solution to the following problem:

$$\begin{aligned} \partial_s W + \frac{c}{a(x, \mathbf{z})} \partial_x W + \frac{1}{a(x, \mathbf{z})} e^{-i\tau} r(e^{i\tau} W) &= -\frac{1}{\varepsilon} \partial_\tau W, \\ W(0, x, \mathbf{z}, \tau) = V(0, x, \mathbf{z}, \tau) &= u_{in}(x, \mathbf{z}) + \frac{\varepsilon}{a(x, \mathbf{z})} \left[\mathcal{G}(0, u_{in}, \mathbf{z}) - \mathcal{G}(\tau, u_{in}, \mathbf{z}) \right], \\ \text{with } \mathcal{G}(\tau, u_{in}, \mathbf{z}) &= \mathcal{L}^{-1}(\mathcal{I} - \Pi)[e^{-i\tau} r(e^{i\tau} u_{in}(x, \mathbf{z}))]. \end{aligned} \tag{2.35}$$

We then have the following result for W .

Proposition 2.1. *Let W be the solution of (2.35) on $[0, \bar{T}]$, $\bar{T} > 0$, with periodic boundary condition in x and τ . Then, up to the second order derivative in s , and arbitrary order in x and \mathbf{z} derivatives of W are bounded uniformly in $\varepsilon \in [0, 1]$, that is, $\exists C > 0$ independent of ε such that, $\forall s \in [0, \bar{T}]$*

$$\|\partial_s^p \partial_x^q \partial_{\mathbf{z}}^r W(s)\|_{L^\infty_x(L^2(\pi(\mathbf{z}) d\mathbf{z}))} \leq C, \quad \text{for } p = 0, 1, 2, \quad \text{and } q, r \in \mathbb{N}.$$

This proposition can be deduced from Proposition 2.5 of [8] in which we replace x by (x, \mathbf{z}) . In fact, the W -equation (2.35) was introduced in [8] to prove the uniform in ε regularity and convergence of the NGO-based method. Note in particular that the high order derivatives in x and \mathbf{z} are uniformly bounded at *any* order with respect to ε although the initial data for W is only prepared at the first order in ε . This guarantees the uniform accuracy in \mathbf{z} and x , that is in particular

$$\left\| W - \sum_{j=1}^K \tilde{W}_j \tilde{\psi}_j \right\|_{L^2(\pi(\mathbf{z}) d\mathbf{z})} \leq \frac{C}{K^q}, \quad \forall q \text{ positive integer,}$$

where C is a positive constant which is independent of ε , and q depends only on the regularity in \mathbf{z} of the initial data $u_{in}(x, \mathbf{z})$. Thus one can choose K independent of ε .

To summarize, to obtain a spectral accuracy in \mathbf{z} at any order uniformly in ε , one has to solve equation (2.35) satisfied by W (instead of the equation on V) and then recover V by formula (2.34). Note that the mapping $t \mapsto S(t, x, \mathbf{z})$ is a increasing function in t for any fixed (x, \mathbf{z}) . Of course, this needs an interpolation in time to get back to the t variable for V .

2.5.1. The gPC-SG-N2 method

The above discussion motivates us to design the following new scheme, denoted by gPC-SG-N2 in the sequel.

The gPC system for solving the equation for S is the same as in Section 2.3.1. For the equation on W , we insert the gPC-SG ansatz

$$W(s, x, \tau, \mathbf{z}) \approx \sum_{|\mathbf{k}| \leq P} W_{\mathbf{k}}(s, x, \tau) \psi_{\mathbf{k}}(\mathbf{z}) = \sum_{j=1}^K \tilde{W}_j(s, x, \tau) \tilde{\psi}_j(\mathbf{z})$$

into (2.35) and conduct the Galerkin projection to get

$$\partial_s \vec{W} + c(x) A^*(x) \partial_x \vec{W} + e^{-i\tau} \vec{\gamma}^*(e^{i\tau} W) = -\frac{1}{\varepsilon} \partial_\tau \vec{W}, \tag{2.36}$$

where A^* is the symmetric and positive-definite matrix given by

$$A_{ij}^*(x) = \int_{I_{\mathbf{z}}} \frac{1}{a(x, \mathbf{z})} \psi_i(\mathbf{z}) \psi_j(\mathbf{z}) \pi(\mathbf{z}) \, d\mathbf{z},$$

and

$$\vec{W}(s, x, \tau) = \left(\tilde{W}_1(s, x, \tau), \dots, \tilde{W}_K(s, x, \tau) \right)^T.$$

The j th component $\tilde{\gamma}_j^*$ of the vector $\vec{\gamma}^*$ is ,

$$\tilde{\gamma}_j^*(e^{i\tau}W) = \int_{I_{\mathbf{z}}} \frac{1}{a(x, \mathbf{z})} r(e^{i\tau}W) \tilde{\psi}_j(\mathbf{z}) \pi(\mathbf{z}) \, d\mathbf{z}, \quad \text{for } j = 1, \dots, K, \tag{2.37}$$

which is computed by the Gauss-quadrature formula. The initial data for W is the same as for V : $W(0, x, \tau, \mathbf{z}) = V(0, x, \tau, \mathbf{z})$, which is shown in Section 2.3.1.

2.5.2. The fully discrete gPC-SG-N2 method

Let the final time be T . Define the grid points in space $x_j, j = 0, 1, \dots, N_x$. As discussed in (2.19), to recover the solution u , one needs a trigonometric interpolation on $\tau = \frac{S(T, x_j, \mathbf{z}^{(l)})}{\varepsilon}$, for each quadrature points $\mathbf{z}^{(l)}, l = 1, \dots, N_s$,

$$u(T, x_j, \mathbf{z}^{(l)}) \approx V\left(T, x_j, \tau = \frac{S(T, x_j, \mathbf{z}^{(l)})}{\varepsilon}, \mathbf{z}^{(l)}\right),$$

then one can compute the mean and standard deviation of u at (T, x_j) in the random space,

$$\mathbb{E}(u)(T, x_j) = \sum_{l=1}^{N_s} u(T, x_j, \mathbf{z}^{(l)}) \omega_l, \quad \text{SD}(u)(T, x_j) = \left(\sum_{l=1}^{N_s} |u(T, x_j, \mathbf{z}^{(l)})|^2 \omega_l - (\mathbb{E}(u)(T, x_j))^2 \right)^{1/2},$$

where ω_l are the corresponding quadrature weights. After obtaining the values of S at $(T, x_j, \mathbf{z}^{(l)})$ for all j, l , let

$$S^* = \max_{j,l} \left\{ S(T, x_j, \mathbf{z}^{(l)}) \right\}.$$

We choose $s \in [0, S^*]$ to be the time domain for computing W . Define the time discretization of W as s_l , for $l = 0, 1, \dots, L$, with time step Δs and the total number of time steps $L = \left\lceil \frac{S^*}{\Delta s} \right\rceil + 1$.

To solve the equation on \vec{W} , knowing \vec{S} , we start by the initial value $\vec{W}(0, x, \tau) = \vec{V}(0, x, \tau)$ given by (2.29) at $x = x_j$. Then the system is advanced in time by a simple time-splitting algorithm as explained for the deterministic case in Section 2.2. The nonlinear part (the $\vec{\gamma}^*$ term) and the transport part are treated in a similar way as in Section 2.2. For the oscillatory part, we use the backward Euler method in time,

$$\frac{\vec{W}_j^{n+1} - \vec{W}_j^n}{\Delta s} = -\frac{1}{\varepsilon} \partial_\tau \vec{W}_j^{n+1}, \tag{2.38}$$

where \vec{W}_j^n is an approximation of $\vec{W}(n\Delta s, x_j)$. Let $\hat{W}_j^n(\zeta)$ be the Fourier transform of \vec{W}_j^n in the periodic variable τ , where ζ is the Fourier variable. The spectral method is used to discretize the τ -derivative, then (2.38) becomes

$$\vec{W}_j^{n+1} = \left(I + i\zeta \frac{\Delta s}{\varepsilon} I \right)^{-1} \vec{W}_j^n.$$

Note that the matrix $I + i\zeta \frac{\Delta s}{\varepsilon} I$ has non-zero eigenvalues, thus is invertible.

– **The interpolation step**

To find the values of V at time T , since $V(T, x_j, \tau_k, \mathbf{z}^{(l)}) = W(S(T, x_j, \mathbf{z}^{(l)}), x_j, \tau_k, \mathbf{z}^{(l)})$, one uses linear interpolation to find W at $(S(T, x_j, \mathbf{z}^{(l)}), x_j, \tau_k, \mathbf{z}^{(l)})$, for $l = 1, \dots, N_s$.

We search for the interval $[s_{n_l}, s_{n_l+1}]$ that contains $S(T, x_j, \mathbf{z}^{(l)})$. Denote $S(T, x_j, \mathbf{z}^{(l)}) = s^\dagger$, $s_{n_l} = s^{(1)}$, $s_{n_l+1} = s^{(2)}$, $W(s_{n_l}) = W^{(1)}$, $W(s_{n_l+1}) = W^{(2)}$, then by the Lagrange interpolation formula,

$$W(s^\dagger) = W^{(1)} \frac{s^\dagger - s^{(2)}}{s^{(1)} - s^{(2)}} + W^{(2)} \frac{s^\dagger - s^{(1)}}{s^{(2)} - s^{(1)}},$$

which gives $V(T, x_j, \tau_k, \mathbf{z}^{(l)}) = W(s^\dagger, x_j, \tau_k, \mathbf{z}^{(l)})$.

Remark 2.2. Compared to gPC-SG-N1, the transport step is more costly since one has to multiply by the matrix A^* . If $a = O(1)$, then the CFL condition for the transport equation requires just $\Delta t = O(\Delta x)$ thus independent of ε . However, for avoided crossing, typically $a(x, \mathbf{z}) = \mathcal{O}(\sqrt{\varepsilon})$ for some region of x , thus the eigenvalue of A^* are of $\mathcal{O}(1/\sqrt{\varepsilon})$, thus an explicit time discretization of the transport step will require $\Delta t = \mathcal{O}(\sqrt{\varepsilon}\Delta x)$, further increasing the computational cost. One may use implicit time discretization in the transport step. This will be studied in our future research.

2.6. Numerical tests for the 1D scalar equation

For numerical comparison, we also use the stochastic collocation (SC) method [26, 27]. Let $\{\mathbf{z}^{(j)}\}_{j=1}^{N_c} \subset I_{\mathbf{z}}$ be the set of collocation nodes, N_c the number of samples. For each fixed individual sample $\mathbf{z}^{(j)}$, $j = 1, \dots, N_c$, one applies the deterministic solver to the deterministic equations as in [8], obtains the solution ensemble $u_j(t, x) = u(t, x, \mathbf{z}^{(j)})$, then adopts an interpolation approach to construct a gPC approximation, such as

$$u(t, x, \mathbf{z}) = \sum_{j=1}^{N_c} u_j(t, x) l_j(\mathbf{z}),$$

where $l_j(\mathbf{z})$ depends on the construction method. The Lagrange interpolation method is used here by choosing $l_j(\mathbf{z}^{(i)}) = \delta_{ij}$. Depending on whether the direct or NGO-based method is used for the deterministic method, we will have the gPC-SC-D and gPC-SG-N1, gPC-SG-N2 methods.

Example 2.3. We consider the numerical example in [8], with a involving a 1D random variable z that follows a uniform distribution,

$$r(u) = u^2 / (u^2 + 2|u|^2), \quad c(x) = \cos^2(x), \quad a(x, z) = (3/2 + \cos(2x))(1 + 0.5z) > 0,$$

and the non-oscillatory initial data given by

$$u(0, x) = 1 + \frac{1}{2} \cos(2x) + i \left[1 + \frac{1}{2} \sin(2x) \right], \quad x \in [-\pi/2, \pi/2].$$

In the following tests, for all the reference solutions obtained from gPC-SC-D method, $N_c = 64$, $N_g = 32$ quadrature points are used. In gPC-SG-N1 and gPC-SG-N2 methods, N_s stands for the number of quadrature points used in the final reconstruction step (to get u from V or W). We choose $N_\tau = 16$ in all the tests.

Figures 1 and 2 demonstrate how ε affects the choices of K for gPC-SG-D. Here the gPC-SC-D, computed with very small Δt and Δx , is used to obtain the reference solutions. For gPC-SG-D, we also use very small Δx and Δt , in order to concentrate on effect of ε on K . We output the solution at $t = 0.1$. In Figure 1, for $\varepsilon = 1$ and 0.1 , one can use $K = 4$. However, for $\varepsilon = 0.01$, neither $K = 4$ nor $K = 8$ gives the correct solutions, especially around the center of the domain. One starts to see satisfactory numerical solutions when $K = 10$. For $\varepsilon = 0.005$ one needs to use $K = 20$, see Figure 2.

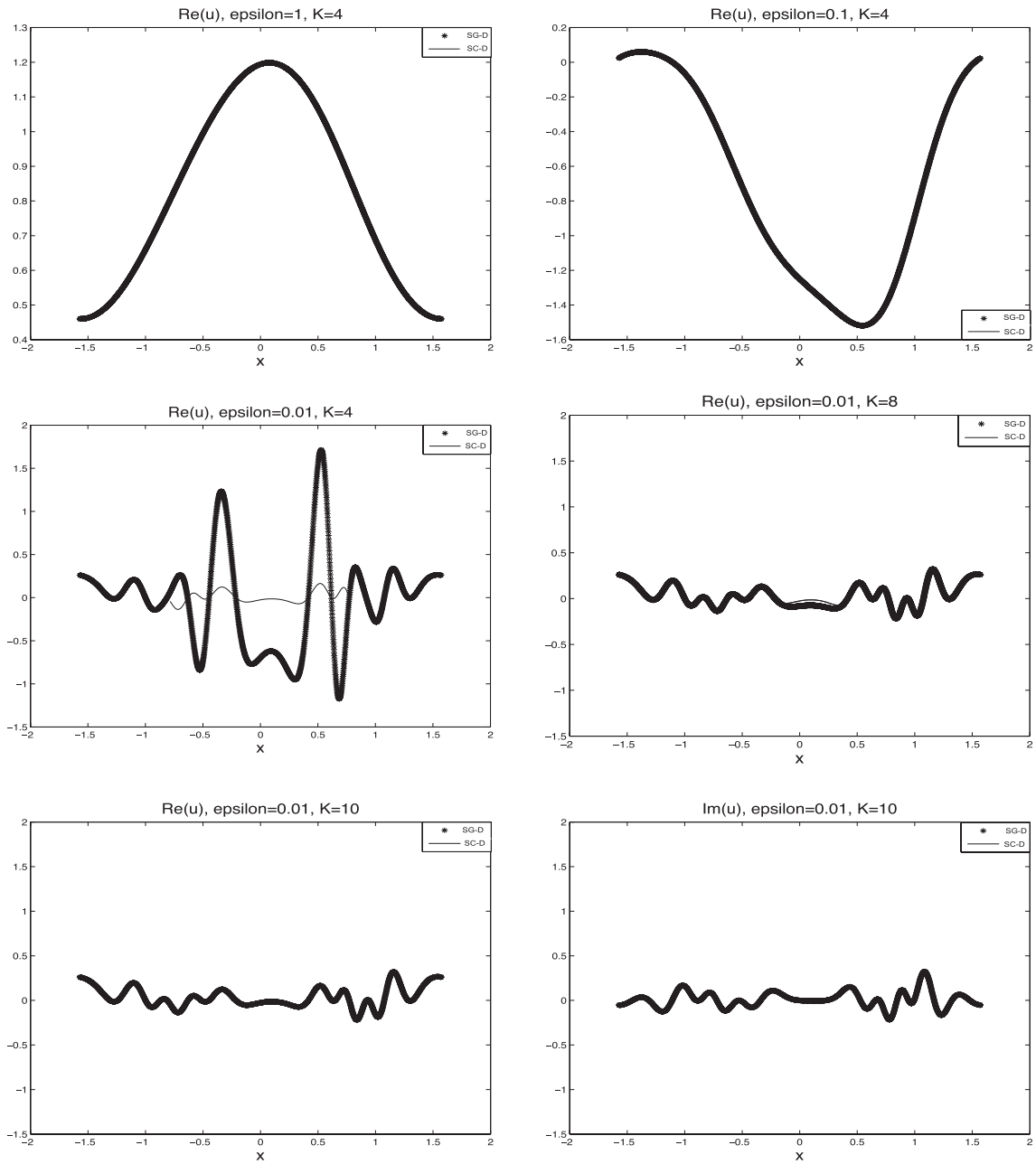


FIGURE 1. Example 2.3. Mean of real parts of u at $t = 0.1$, $\epsilon = 1, 0.1$ and 0.01 . $N_x = 2000$, $\Delta t = 10^{-5}$. Stars: gPC-SG-D with $K = 4$. Solid lines: reference solution by gPC-SC-D.

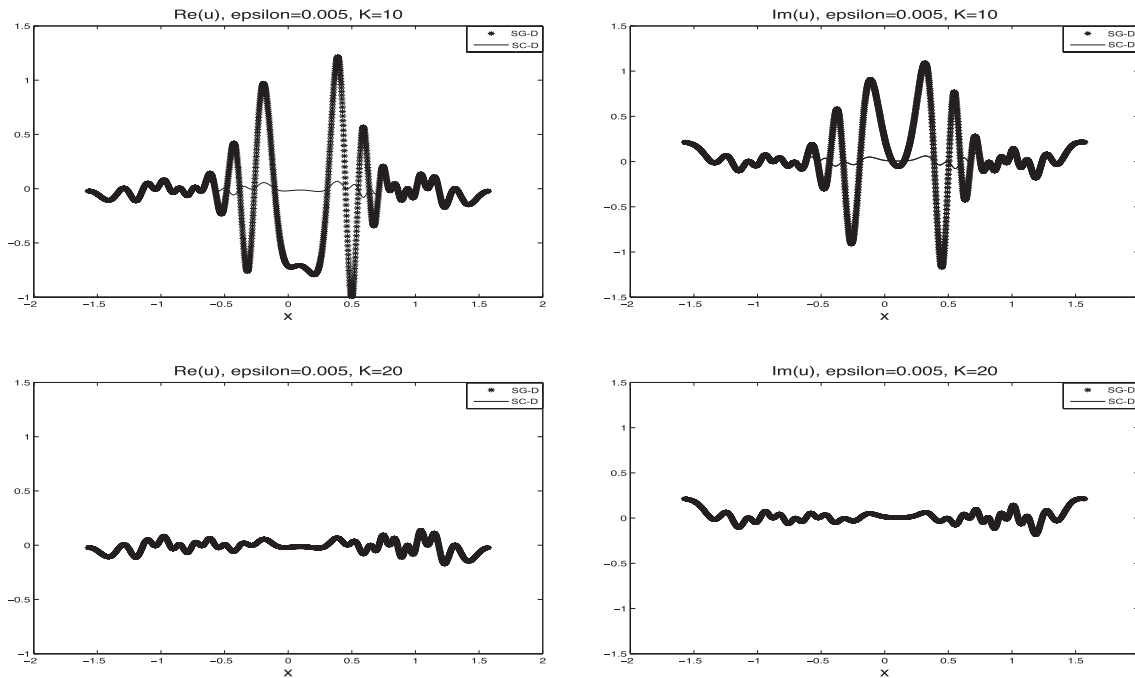


FIGURE 2. Example 2.3. Mean of real parts of u at $t = 0.1$, $\varepsilon = 5 \times 10^{-3}$. $N_x = 2000$, $\Delta t = 10^{-5}$. Stars: gPC-SG-D. Solid lines: reference solution by gPC-SC-D.

Figures 3 and 4 compare mean of the solutions of gPC-SG-N1 and gPC-SG-N2 for $\varepsilon = 0.01$, and $\varepsilon = 0.005$ respectively. We take small ε and use gPC-SC-D to fully resolve the oscillations (to serve as a reference solution). One can observe from Figure 4 that gPC-SG-N2 is able to capture correctly the solution (its mean and standard deviation) at mesh points with $\Delta x, \Delta t$ much larger than ε and $K = 4$. For the same grids, gPC-SG-N1 is a bit off near $x = 0$. If one uses a much finer spatial size $\Delta x = \pi/1000$, gPC-SG-N1 becomes more accurate but still is a bit off near $x = 0$, as shown in the second row of Figure 3.

Figure 5 and 6 perform two-dimensional random variable tests. We use the same data in Example 2.3, while change $a(x, \mathbf{z}) = 1 + 0.6z_1 + 0.3z_2$ with $\mathbf{z} := (z_1, z_2)$ following the uniform distribution on $[-1, 1]$ in Figure 5, and $a(x, \mathbf{z}) = 1 + 0.4 \sin(z_1) + 0.2 \cos(z_2)$ with $\mathbf{z} := (z_1, z_2)$ following the normal Gaussian distribution. The discretization parameters used in the gPC-SG-N2 method are: $\Delta x = \pi/32$, $\Delta t = 0.005$, $K = 6$, $N_s = 144$, $\varepsilon = 0.025$ in Figure 5 and $\varepsilon = 0.5$ in Figure 6. According to (2.2), there are $\binom{K+2}{K} = 21$ basis functions in the gPC method. When comparing the solutions of gPC-SG-N2 and gPC-SG-D, the mean values are captured quite accurately, however the accuracy of the standard deviation is slightly inferior to the accuracy of the mean. It can be observed even in the one-dimensional random variable case, for example in Figure 7 below. This is not surprising, since by definition (2.4) for the gPC methods, the mean is u_1 , while the error of standard deviation is an accumulation of errors in u_j for $2 \leq j \leq K$.

Some comparisons between the gPC-SG-N1 and gPC-SG-N2 methods are shown in Figure 7 in the case of $\varepsilon = 3 \times 10^{-3}$. We first plot the mean of real part of u (zoomed in solutions) with $K = 4$, $N_s = 144$ in gPC-SG-N1 and gPC-SG-N2 and observes that gPC-SG-N2 can capture the correct mean and standard deviation, while gPC-SG-N1 can not. Using $K = 4$, $N_s = 800$ in gPC-SG-N1 still does not give the good result, and further increasing the gPC order ($K = 16$) enables the mean and standard deviation of $\text{Re}(u)$ to capture the

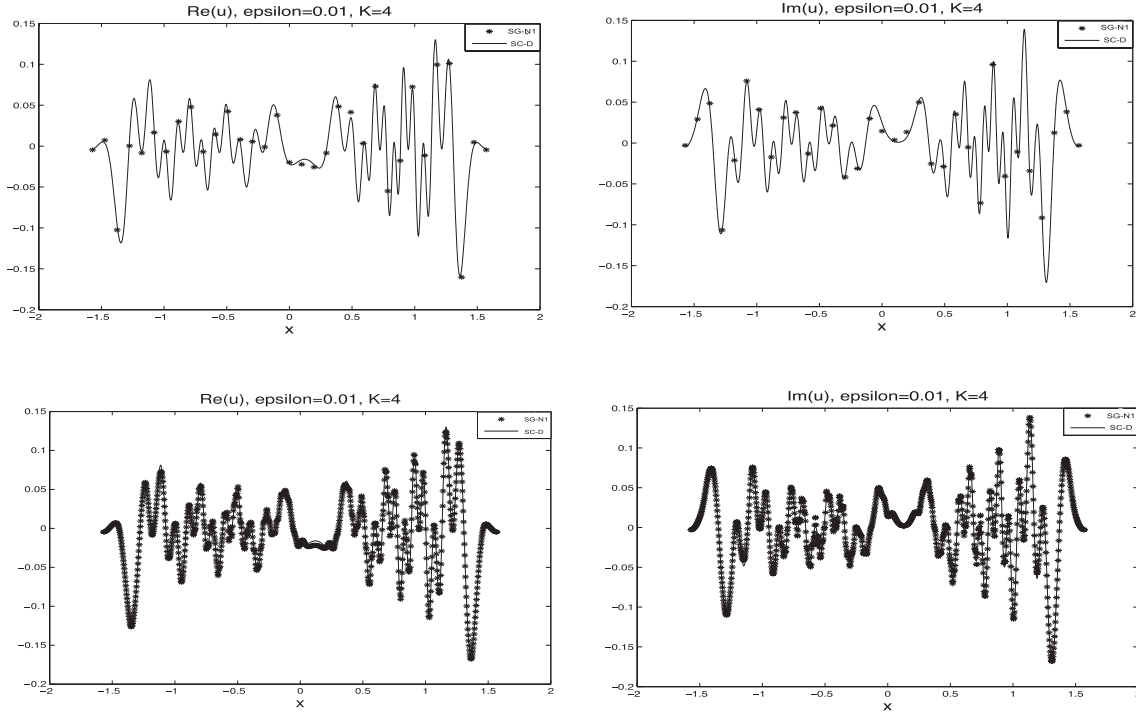


FIGURE 3. Example 2.3. Mean of real and imaginary parts of u at $t = 0.25$, $\varepsilon = 0.01$. $\Delta x = \pi/32$, $\Delta t = 0.01$ for the first row (gPC-SG-N1), and $\Delta x = \pi/1000$, $\Delta t = 10^{-4}$ for the second row (gPC-SG-N1). $\Delta x = \pi/1000$, $\Delta t = 5 \times 10^{-5}$ (gPC-SC-D). Stars: gPC-SG-N1 with $K = 4$. Solid lines: reference solution by gPC-SC-D.

oscillations. Thus gPC-SG-N2 does not require larger K or N_s when ε is small, whereas larger K and N_s are needed in gPC-SG-N1.

Note that for the deterministic problem, the uniform convergence in space and time was already proved rigorously in [8], here we will conduct a numerical experiment to check the uniform convergence in the random space. Figure 8 shows a semi-log plot of the l^∞ errors for mean and standard deviation of $\text{Re}(u)$ and $\text{Im}(u)$ of gPC-SG-N2 with respect to varying gPC order K at $T = 0.1$, with two different ε 's, namely $\varepsilon = 0.1$ (left) and $\varepsilon = 5 \times 10^{-3}$ (right). In both cases, t errors quickly decay when one increases K , and then saturate at modest K since the errors arising from the temporal, spatial and τ discretizations start to dominate. Therefore, we demonstrate a fast exponential convergence with respect to K , for both ε , indicating that one can choose K independent of ε in gPC-SG-N2.

3. A SEMICLASSICAL SURFACE HOPPING MODEL WITH RANDOM INPUTS

We consider a semiclassical surface hopping model in one dimension in space and momentum, with random inputs,

$$\begin{cases} \partial_t f^+ + p \partial_x f^+ - \partial_x(U + E) \partial_p f^+ = \bar{b}^i f^i + b^i \bar{f}^i, \\ \partial_t f^- + p \partial_x f^- - \partial_x(U - E) \partial_p f^- = -\bar{b}^i f^i - b^i \bar{f}^i, \\ \partial_t f^i + p \partial_x f^i + \partial_x U \partial_p f^i = -i \frac{2E}{\varepsilon} f^i + b^i (f^- - f^+) + (b^+ - b^-) f^i, \end{cases} \quad (3.1)$$

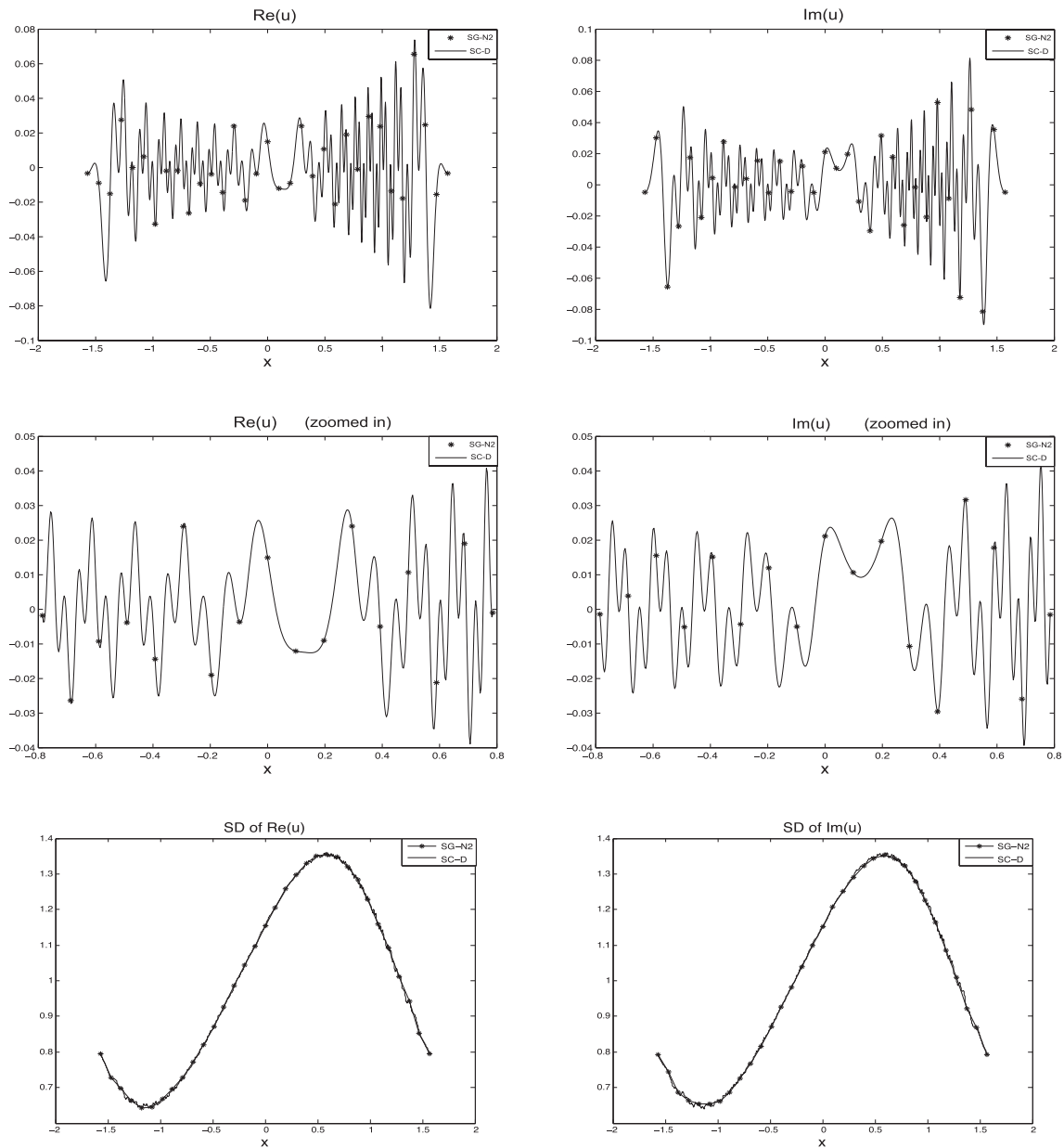


FIGURE 4. Example 2.3. Mean and standard deviation of real and imaginary parts of u and their zoomed in solutions at $t = 0.25$, $\varepsilon = 5 \times 10^{-3}$, $\Delta x = \pi/32$, $\Delta t = 0.01$, $K = 4$ (gPC-SG-N2), and $\Delta x = \pi/1000$, $\Delta t = 5 \times 10^{-5}$ (gPC-SC-D). Stars: gPC-SG-N2. Solid lines: reference solution by gPC-SC-D.

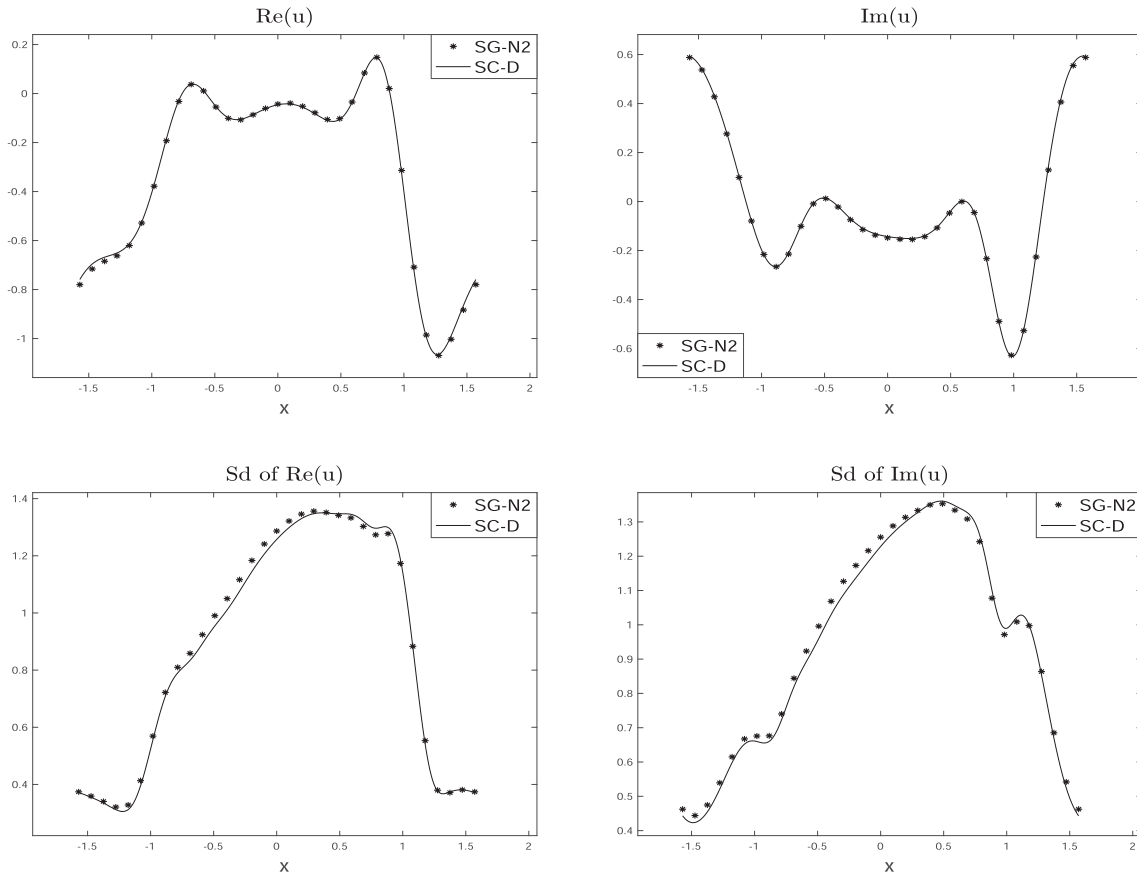


FIGURE 5. Example 2.3 with a two-dimensional random variable \mathbf{z} and $a(x, \mathbf{z}) = 1 + 0.6z_1 + 0.3z_2$ with $\mathbf{z} := (z_1, z_2)$ following the uniform distribution on $[-1, 1]$. Mean and standard deviation of real and imaginary parts of solution u at $t = 0.07$, $\varepsilon = 0.025$. We use $\Delta x = \pi/32$, $\Delta t = 0.005$, $K = 6$ (gPC-SG-N2), and $\Delta x = \pi/500$, $\Delta t = 10^{-4}$ (gPC-SC-D). Stars: gPC-SG-N2. Solid lines: reference solution by gPC-SC-D.

where $(f^+(t, x, p, \mathbf{z}), f^-(t, x, p, \mathbf{z}), f^i(t, x, p, \mathbf{z})) \in \mathbb{R}_+ \times \mathbb{R}_+ \times \mathbb{C}$, $(t, x, p) \in \mathbb{R}_+ \times \mathbb{R} \times \mathbb{R}$, and $b^\pm \in \mathbb{C}$, $b^i \in \mathbb{C}$, $E = E(x, \mathbf{z}) \in \mathbb{R}$ are given functions depending on (x, p, \mathbf{z}) .

This system is equipped with initial conditions $f^\pm(0, x, p) = f_{in}^\pm(x, p)$ and $f^i(0, x, p) = f_{in}^i(x, p)$.

We also define the zeroth moments of $f^{\pm,i}$ as

$$\rho^{\pm,i}(t, x, \mathbf{z}) = \int_{\mathbb{R}} f^{\pm,i}(t, x, p, \mathbf{z}) dp.$$

Here ρ^\pm denote the densities of particles in the two bands.

This model, introduced in [4], was a semiclassical approximation to the nucleonic Schrödinger system that arises from the Born–Oppenheimer approximation with *non-adiabatic* phenomenon, in which particles can “hop” from one potential energy surface to the other ones. Here f^\pm stand for the particle density distributions in the two energy surfaces respectively, while f^i is the off-diagonal entry of the semiclassical Wigner matrix. The right hand side of the system describes the interband transition between different potential energy surfaces with the *energy gap* $\Delta E = 2E$, which can be random in reality. In particular, the so-called *avoided crossing* corresponds to where the minimum energy gap of order $\sqrt{\varepsilon}$.

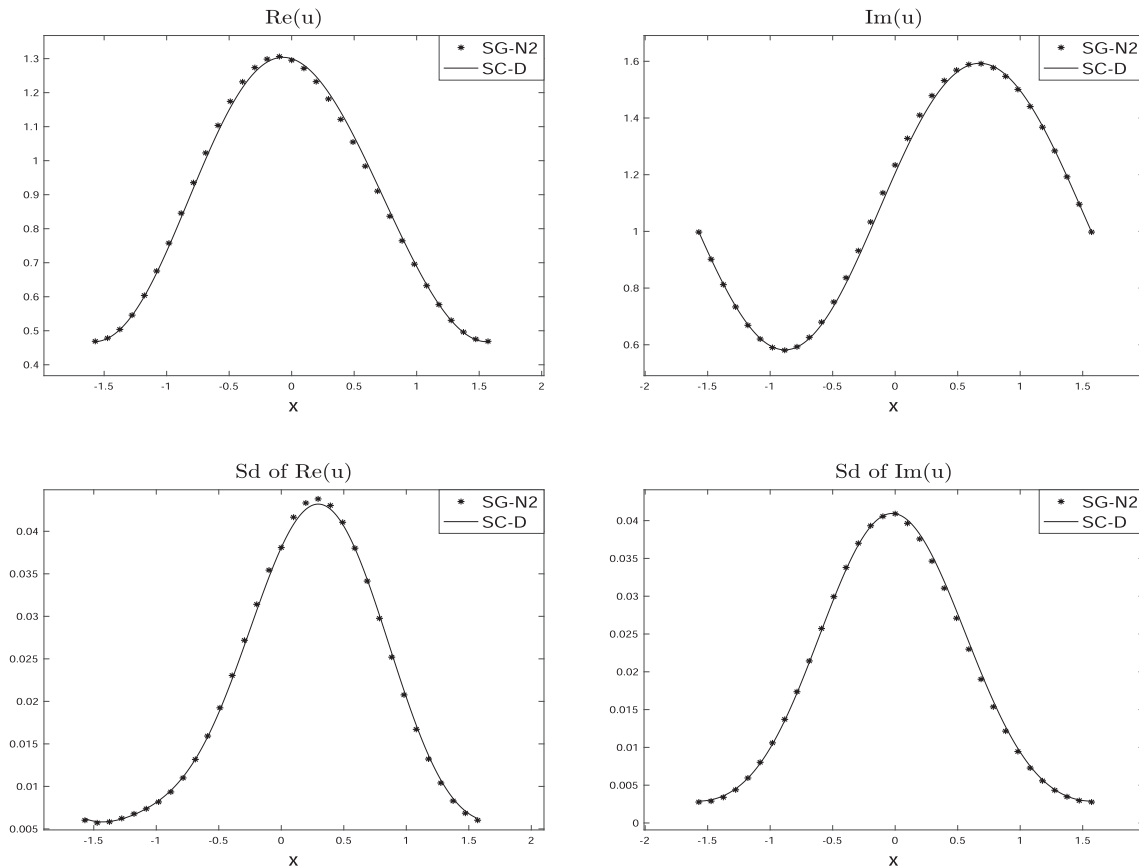


FIGURE 6. Example 2.3 with a two-dimensional random variable \mathbf{z} and $a(x, \mathbf{z}) = 1 + 0.4 \sin(z_1) + 0.2 \cos(z_2)$ with $\mathbf{z} := (z_1, z_2)$ following the normal Gaussian distribution. Mean and standard deviation of real and imaginary parts of solution u at $t = 0.03$, $\varepsilon = 0.5$. We use $\Delta x = \pi/32$, $\Delta t = 0.005$, $K = 6$ (gPC-SG-N2), and $\Delta x = \pi/500$, $\Delta t = 10^{-4}$ (gPC-SC-D). Stars: gPC-SG-N2. Solid lines: reference solution by gPC-SC-D.

3.1. The direct method

In this part and the following sections, we assume that the function $E(x, \mathbf{z})$ is given and random, whereas no randomness is introduced to the initial function.

Introduce the following matrix

$$\mathcal{A} = \text{diag}(-\partial_x(U + E), \partial_x(U - E), \partial_x U, \partial_x U), \tag{3.2}$$

The specific form of b^i depends on the potential matrix in the nucleonic Schrödinger equation. Here we consider $b^i = b^i(x, p) \in \mathbb{R}$, $b^\pm = 0$, which correspond to two specific potential matrices considered in [4]. Let

$$B = \begin{pmatrix} 0 & 0 & 2b^i & 0 \\ 0 & 0 & -2b^i & 0 \\ -b^i & b^i & 0 & 2E/\varepsilon \\ 0 & 0 & -2E/\varepsilon & 0 \end{pmatrix},$$

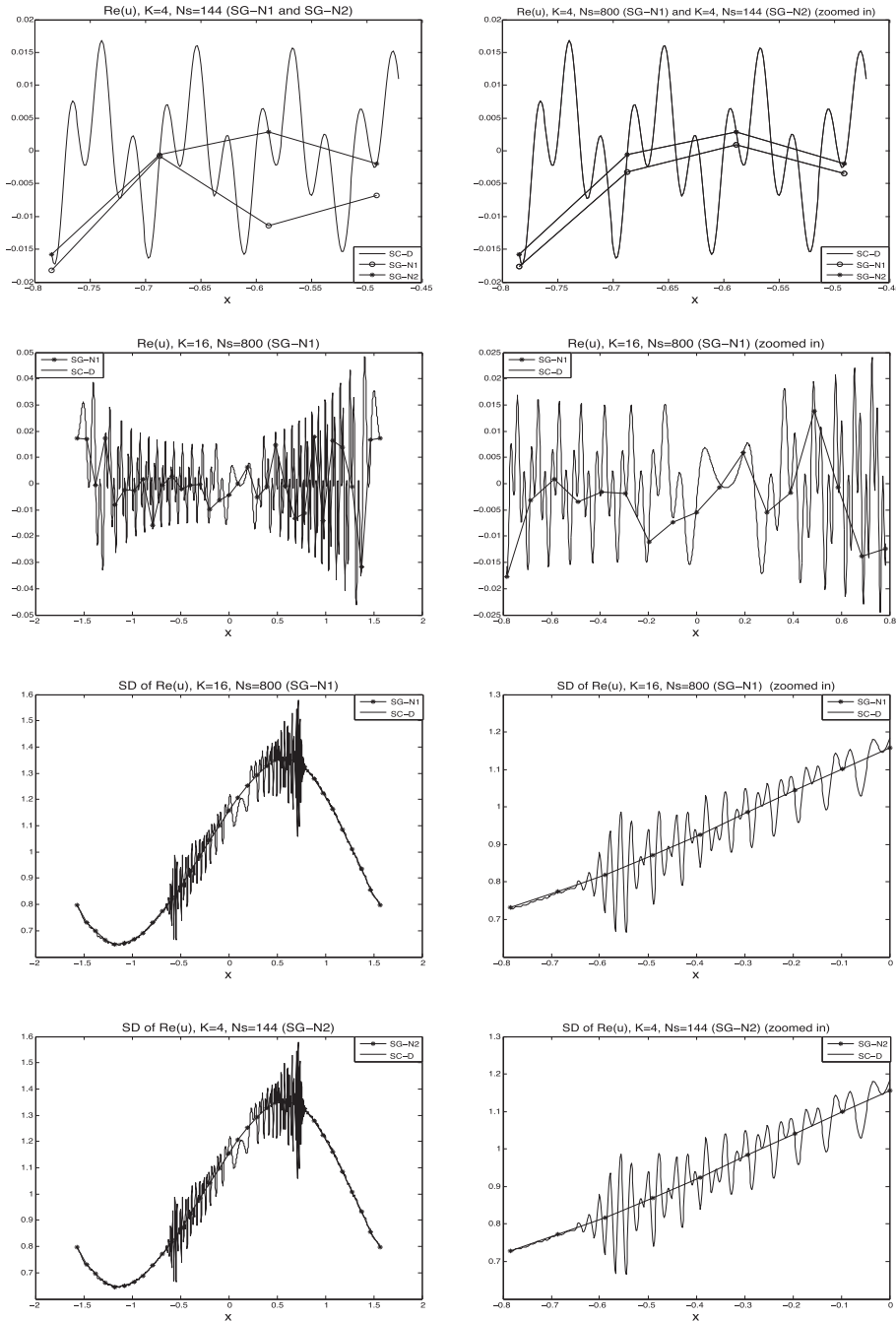


FIGURE 7. Example 2.3. Mean (first two rows) and standard deviation (last row) of real parts of u (and their zoomed in solutions) at $t = 0.25$, $\varepsilon = 3 \times 10^{-3}$. $\Delta x = \pi/32$, $\Delta t = 0.01$ (gPC-SG-N1 and gPC-SG-N2), $\Delta x = \pi/2000$, $\Delta t = 5 \times 10^{-5}$ (gPC-SC-D). Solid lines: reference solution by gPC-SC-D.

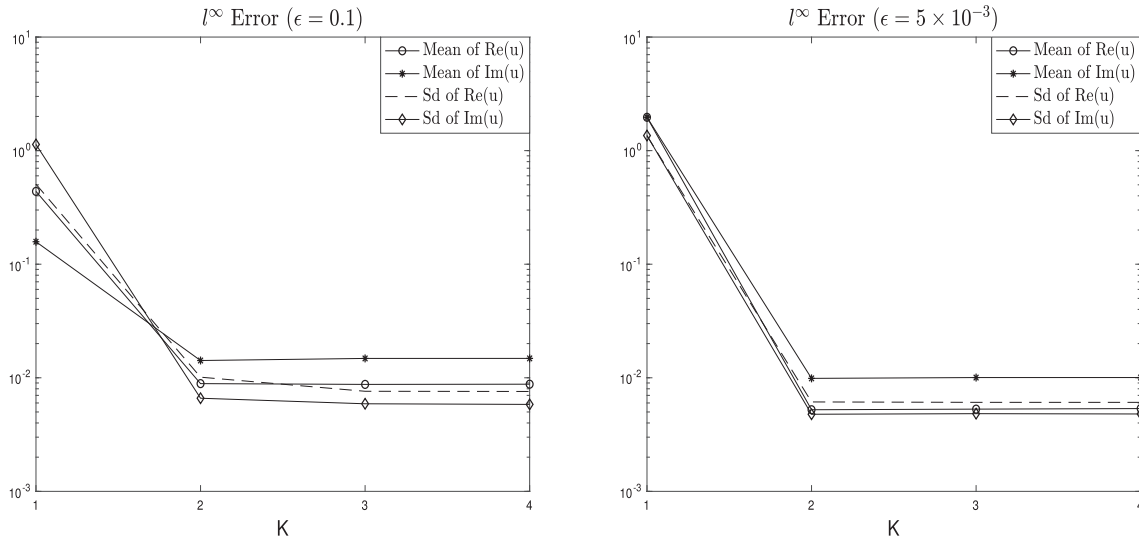


FIGURE 8. Plot of the l^∞ errors for mean and standard deviation of $\text{Re}(u)$ using gPC-SG-N2 with respect to different gPC orders. $T = 0.1$, $\varepsilon = 0.1$ (left) and $\varepsilon = 5 \times 10^{-3}$ (right). $\Delta x = \pi/64$, $\Delta t = 0.02$ compared with the (well-resolved) reference solutions computed by using (gPC-SC-D) with $\Delta x = \pi/1024$, $\Delta t = 5 \times 10^{-5}$.

and write $f = (f^+, f^-, g := \text{Re}(f^i), h := \text{Im}(f^i)) \in \mathbb{R}^4$, then (3.1) can be written as

$$\partial_t f + p\partial_x f + \mathcal{A}\partial_p f = Bf, \tag{3.3}$$

which will be solved using simple operator splitting method:

- (1) Solve $\partial_t f + p\partial_x f = 0$ using spectral method in space and exact integration in time.
- (2) Solve $\partial_t f + \mathcal{A}\partial_p f = 0$ using spectral method in velocity and exact integration in time.
- (3) Solve $\partial_t f = Bf$ to be specified below.

The first two steps are the same for both the direct and the NGO-based method (to be introduced in Sect. 3.2). For step 3, since the matrix B now involves randomness, instead of solving the whole system exactly in time, we use a Crank–Nicolson method in time coupled with a substitution method to save computations. More precisely, we have

$$\frac{f^{+,n+1} - f^{+,n}}{\Delta t} = \frac{1}{2}2b^i (g^n + g^{n+1}), \tag{3.4}$$

$$\frac{f^{-,n+1} - f^{-,n}}{\Delta t} = -\frac{1}{2}2b^i (g^n + g^{n+1}), \tag{3.5}$$

$$\frac{g^{n+1} - g^n}{\Delta t} = \frac{1}{2} \left[-b^i f^{+,n} + b^i f^{-,n} + \frac{2E}{\varepsilon} h^n - b^i f^{+,n+1} + b^i f^{-,n+1} + \frac{2E}{\varepsilon} h^{n+1} \right], \tag{3.6}$$

$$\frac{h^{n+1} - h^n}{\Delta t} = -\frac{1}{2} \frac{2E}{\varepsilon} (g^n + g^{n+1}). \tag{3.7}$$

We used classical notations for the time approximation, for example $f^{+,n} \approx f^+(t_n)$. From (3.4), one solves $f^{+,n+1}$ in terms of g^{n+1} , and then substitute it into (3.6) to get g^{n+1} ,

$$\begin{aligned} & \left[1 + (b^i)^2(\Delta t)^2 + \frac{E^2}{\varepsilon^2}(\Delta t)^2 \right] g^{n+1} \\ & = g^n + \Delta t \left[-b^i f^{-,n} + b^i f^{-,n} + \frac{2E}{\varepsilon} h^n - (b^i)^2 \Delta t g^n - \frac{E^2}{\varepsilon^2} \Delta t g^n \right]. \end{aligned} \tag{3.8}$$

Then the other unknowns $f^{\pm,n+1}$ and h^{n+1} can be obtained from (3.4), (3.6) and (3.7).

3.2. The NGO based method

We first review the NGO-based method introduced in [8], wherein deterministic $E = E(x)$ and deterministic initial data is considered.

We introduce the augmented unknowns $(F^\pm, G, H)(t, x, p, \tau)$ satisfying

$$f^\pm(t, x, p) = F^\pm(t, x, p, S(t, x, p)/\varepsilon), \quad f^i(t, x, p) = e^{iS(t, x, p)/\varepsilon} (G + iH)(t, x, p, S(t, x, p)/\varepsilon). \tag{3.9}$$

The phase function $S(t, x, p)$ is designed to follow the main oscillations in the model. Assume periodicity in S/ε , S solves

$$\partial_t S + p \partial_x S + \partial_x U \partial_p S = 2E, \quad S(0, x, p) = 0. \tag{3.10}$$

Then F^\pm, G and H solve

$$\begin{cases} \partial_t F^+ + p \partial_x F^+ - \partial_x(U + E) \partial_p F^+ = -\frac{\mathcal{E}^+}{\varepsilon} \partial_\tau F^+ + 2b^i(G \cos \tau + H \sin \tau), \\ \partial_t F^- + p \partial_x F^- - \partial_x(U - E) \partial_p F^- = -\frac{\mathcal{E}^-}{\varepsilon} \partial_\tau F^- - 2b^i(G \cos \tau + H \sin \tau), \\ \partial_t G + p \partial_x G + \partial_x U \partial_p G = -\frac{2E}{\varepsilon} \partial_\tau G + b^i(F^- - F^+) \cos \tau, \\ \partial_t H + p \partial_x H + \partial_x U \partial_p H = -\frac{2E}{\varepsilon} \partial_\tau H + b^i(F^- - F^+) \sin \tau, \end{cases} \tag{3.11}$$

where we denoted

$$\mathcal{E}^\pm(t, x, p) = 2E - \partial_x(2U \pm E) \partial_p S. \tag{3.12}$$

The well-prepared initial conditions are given by (see [8])

$$F^+(0, x, p, \tau) = f_{in}^+ - i \frac{\varepsilon}{\mathcal{E}^+} (\bar{b}^i f_{in}^i (1 - e^{-i\tau}) - b^i \bar{f}_{in}^i (1 - e^{i\tau})), \tag{3.13}$$

$$F^-(0, x, p, \tau) = f_{in}^- + i \frac{\varepsilon}{\mathcal{E}^-} (\bar{b}^i f_{in}^i (1 - e^{-i\tau}) - b^i \bar{f}_{in}^i (1 - e^{i\tau})), \tag{3.14}$$

$$G(0, x, p, \tau) = \text{Re}(f_{in}^i) - \frac{\varepsilon}{2E} b^i (f_{in}^+ - f_{in}^-) \sin \tau, \tag{3.15}$$

$$H(0, x, p, \tau) = \text{Im}(f_{in}^i) + \frac{\varepsilon}{2E} b^i (f_{in}^+ - f_{in}^-) (\cos \tau - 1), \tag{3.16}$$

where f_{in}^\pm, f_{in}^i are the initial data of (3.1).

One can also develop the gPC-SG-D and gPC-SG-N1 methods as in Section 2. Since our focus is on gPC-SG-N2, we will just put gPC-SG-N1 and gPC-SG-D in the appendix for future reference.

3.2.1. The gPC-SG-N2 for the system with random inputs

Similar to the discussion in Section 2.4, which allows the gPC order independent of ε , we implement the gPC-SG-N2 scheme. First, one focuses on the approximation of the phase equation (3.10). We insert the approximated solution

$$S(t, x, p, \mathbf{z}) \approx \sum_{j=1}^K \tilde{S}_j(t, x, p) \tilde{\psi}_j(\mathbf{z})$$

into (3.10) and conduct the Galerkin projection. We denote by

$$\vec{S}(t, x, p) = \left(\tilde{S}_1(t, x, p), \dots, \tilde{S}_K(t, x, p) \right)^T,$$

the vector of unknown satisfying

$$\partial_t \vec{S} + p \partial_x \vec{S} + \partial_x U \partial_p \vec{S} = 2 \int_{I_{\mathbf{z}}} E(x, \mathbf{z}) \tilde{\psi}(\mathbf{z}) \pi(\mathbf{z}) \, d\mathbf{z}, \quad \vec{S}(0, x, p) = 0, \tag{3.17}$$

with $\tilde{\psi}(\mathbf{z}) = \left(\tilde{\psi}_1(\mathbf{z}), \dots, \tilde{\psi}_K(\mathbf{z}) \right)$ defined in (2.6). A 4th order Runge–Kutta in time and pseudo-spectral method in space and velocity is used to solve \vec{S} .

Define the augmented functions

$$\begin{aligned} F^+(t, x, p, \tau, \mathbf{z}) &= W_1(S(t, x, p, \mathbf{z}), x, p, \tau, \mathbf{z}), & F^-(t, x, p, \tau, \mathbf{z}) &= W_2(S(t, x, p, \mathbf{z}), x, p, \tau, \mathbf{z}), \\ G(t, x, p, \tau, \mathbf{z}) &= W_3(S(t, x, p, \mathbf{z}), x, p, \tau, \mathbf{z}), & H(t, x, p, \tau, \mathbf{z}) &= W_4(S(t, x, p, \mathbf{z}), x, p, \tau, \mathbf{z}). \end{aligned}$$

Then

$$\partial_t F^+ = \partial_s W_1 \partial_t S, \quad \partial_x F^+ = \partial_s W_1 \partial_x S + \partial_x W_1, \quad \partial_p F^+ = \partial_s W_1 \partial_p S + \partial_p W_1.$$

Denote

$$\mathcal{E}^\pm(t, x, p, \mathbf{z}) = 2E(x, \mathbf{z}) - \partial_x(2U(x) \pm E(x, \mathbf{z})) \partial_p S(t, x, p, \mathbf{z}).$$

By (3.10) and (3.11), we have

$$\begin{cases} \partial_s W_1 + \frac{p}{\mathcal{E}^+(s, x, p, \mathbf{z})} \partial_x W_1 - \frac{\partial_x(U + E)}{\mathcal{E}^+(s, x, p, \mathbf{z})} \partial_p W_1 = -\frac{1}{\varepsilon} \partial_\tau W_1 + \frac{2b^i}{\mathcal{E}^+(s, x, p, \mathbf{z})} (W_3 \cos \tau + W_4 \sin \tau), \\ \partial_s W_2 + \frac{p}{\mathcal{E}^-(s, x, p, \mathbf{z})} \partial_x W_2 - \frac{\partial_x(U - E)}{\mathcal{E}^-(s, x, p, \mathbf{z})} \partial_p W_2 = -\frac{1}{\varepsilon} \partial_\tau W_2 - \frac{2b^i}{\mathcal{E}^-(s, x, p, \mathbf{z})} (W_3 \cos \tau + W_4 \sin \tau), \\ \partial_s W_3 + \frac{p}{2E(x, \mathbf{z})} \partial_x W_3 + \frac{\partial_x U}{2E(x, \mathbf{z})} \partial_p W_3 = -\frac{1}{\varepsilon} \partial_\tau W_3 + \frac{b^i}{2E(x, \mathbf{z})} (W_2 - W_1) \cos \tau, \\ \partial_s W_4 + \frac{p}{2E(x, \mathbf{z})} \partial_x W_4 + \frac{\partial_x U}{2E(x, \mathbf{z})} \partial_p W_4 = -\frac{1}{\varepsilon} \partial_\tau W_4 + \frac{b^i}{2E(x, \mathbf{z})} (W_2 - W_1) \sin \tau. \end{cases} \tag{3.18}$$

How to obtain $\mathcal{E}^\pm(s, x, p, \mathbf{z})$ will be introduced in next Section 3.2.2.

Now we focus on the approximation of the profiles (W_1, W_2, W_3, W_4) . We insert the Galerkin approximation of each component

$$(W_1, W_2, W_3, W_4)(s, x, p, \mathbf{z}) = \sum_{j=1}^K \left((\tilde{W}_1)_j, (\tilde{W}_2)_j, (\tilde{W}_3)_j, (\tilde{W}_4)_j \right) (s, x, p) \tilde{\psi}_j(\mathbf{z}),$$

into (3.18) and conduct the gPC Galerkin projection. Denote the associated gPC coefficients vector of $(\vec{W}_1, \vec{W}_2, \vec{W}_3, \vec{W}_4)$ as previously, for instance for \vec{W}_1 ,

$$\vec{W}_1 = \left((\tilde{W}_1)_1, \dots, (\tilde{W}_1)_K \right)^T. \tag{3.19}$$

Then, we get the gPC system

$$\begin{cases} \partial_s \vec{W}_1 + p \mathcal{J} \partial_x \vec{W}_1 - \mathcal{C} \partial_p \vec{W}_1 = -\frac{1}{\varepsilon} \partial_\tau \vec{W}_1 + 2b^i \mathcal{J} \left(\vec{W}_3 \cos \tau + \vec{W}_4 \sin \tau \right), \\ \partial_s \vec{W}_2 + p \mathcal{L} \partial_x \vec{W}_2 + \mathcal{C} \partial_p \vec{W}_2 = -\frac{1}{\varepsilon} \partial_\tau \vec{W}_2 - 2b^i \mathcal{L} \left(\vec{W}_3 \cos \tau + \vec{W}_4 \sin \tau \right), \\ \partial_s \vec{W}_3 + p \mathcal{H} \partial_x \vec{W}_3 = -\frac{1}{\varepsilon} \partial_\tau \vec{W}_3 + b^i \mathcal{H} \left(\vec{W}_2 - \vec{W}_1 \right) \cos \tau, \\ \partial_s \vec{W}_4 + p \mathcal{H} \partial_x \vec{W}_4 = -\frac{1}{\varepsilon} \partial_\tau \vec{W}_4 + b^i \mathcal{H} \left(\vec{W}_2 - \vec{W}_1 \right) \sin \tau, \end{cases} \tag{3.20}$$

where matrices \mathcal{J} , \mathcal{L} , \mathcal{C} , \mathcal{H} are given by

$$\begin{aligned} \mathcal{J}_{mn}(s, x, p) &= \int_{I_{\mathbf{z}}} \frac{1}{\mathcal{E}^+(s, x, p, \mathbf{z})} \psi_m(\mathbf{z}) \psi_n(\mathbf{z}) \pi(\mathbf{z}) \, d\mathbf{z}, \\ \mathcal{L}_{mn}(s, x, p) &= \int_{I_{\mathbf{z}}} \frac{1}{\mathcal{E}^-(s, x, p, \mathbf{z})} \psi_m(\mathbf{z}) \psi_n(\mathbf{z}) \pi(\mathbf{z}) \, d\mathbf{z}, \\ \mathcal{C}_{mn}(s, x, p) &= \int_{I_{\mathbf{z}}} \frac{\partial_x E(x, \mathbf{z})}{\mathcal{E}^+(s, x, p, \mathbf{z})} \psi_m(\mathbf{z}) \psi_n(\mathbf{z}) \pi(\mathbf{z}) \, d\mathbf{z}, \\ \mathcal{H}_{mn}(x) &= \int_{I_{\mathbf{z}}} \frac{1}{2E(x, \mathbf{z})} \psi_m(\mathbf{z}) \psi_n(\mathbf{z}) \pi(\mathbf{z}) \, d\mathbf{z}. \end{aligned}$$

The initial conditions of $\vec{W}_1, \vec{W}_2, \vec{W}_3, \vec{W}_4$ are

$$\begin{aligned} \vec{W}_1(0, x, p, \tau) &= \vec{F}^+(0, x, p, \tau), & \vec{W}_2(0, x, p, \tau) &= \vec{F}^-(0, x, p, \tau), \\ \vec{W}_3(0, x, p, \tau) &= \vec{G}(0, x, p, \tau), & \vec{W}_4(0, x, p, \tau) &= \vec{H}(0, x, p, \tau). \end{aligned}$$

According to (3.13)–(3.16), by the gPC-SG method, the initial conditions for gPC coefficient vectors $\vec{F}^+, \vec{F}^-, \vec{G}$ and \vec{H} are given by

$$\vec{F}^+(0, x, p, \tau) = f_{in}^+ \vec{Q}_1 - i\varepsilon (\bar{b}^i f_{in}^i (1 - e^{-i\tau}) - b^i \bar{f}_{in}^i (1 - e^{i\tau})) \vec{Q}_2, \tag{3.21}$$

$$\vec{F}^-(0, x, p, \tau) = f_{in}^- \vec{Q}_1 + i\varepsilon (\bar{b}^i f_{in}^i (1 - e^{-i\tau}) - b^i \bar{f}_{in}^i (1 - e^{i\tau})) \vec{Q}_3, \tag{3.22}$$

$$\vec{G}(0, x, p, \tau) = \text{Re}(f_{in}^i) \vec{Q}_1 - \varepsilon b^i (f_{in}^+ - f_{in}^-) \vec{Q}_4 \sin \tau, \tag{3.23}$$

$$\vec{H}(0, x, p, \tau) = \text{Im}(f_{in}^i) \vec{Q}_1 + \varepsilon b^i (f_{in}^+ - f_{in}^-) \vec{Q}_4 (\cos \tau - 1), \tag{3.24}$$

where the vectors $\vec{Q}_1, \vec{Q}_2, \vec{Q}_3, \vec{Q}_4$ are defined by

$$\begin{aligned} \vec{Q}_1 &= \int_{I_{\mathbf{z}}} \psi(\mathbf{z}) \pi(\mathbf{z}) \, d\mathbf{z}, & \vec{Q}_2(0, x, p) &= \int_{I_{\mathbf{z}}} \frac{\psi(\mathbf{z}) \pi(\mathbf{z})}{\mathcal{E}^+(0, x, p, \mathbf{z})} \, d\mathbf{z}, \\ \vec{Q}_3(0, x, p) &= \int_{I_{\mathbf{z}}} \frac{\psi(\mathbf{z}) \pi(\mathbf{z})}{\mathcal{E}^-(0, x, p, \mathbf{z})} \, d\mathbf{z}, & \vec{Q}_4(x) &= \int_{I_{\mathbf{z}}} \frac{\psi(\mathbf{z}) \pi(\mathbf{z})}{2E(x, \mathbf{z})} \, d\mathbf{z}. \end{aligned}$$

3.2.2. The fully discrete scheme for gPC-SG-N2

Monotonicity of S in terms of t

Assume $U = U(x) \in \mathbb{R}$, $E = E(x, \mathbf{z}) > 0$,

$$\partial_t S + p \partial_x S + \partial_x U \partial_p S = 2E(x, \mathbf{z}), \quad S_{in}(x, p, \mathbf{z}) = 0.$$

By the method of characteristics,

$$\frac{dx}{dt} = p, \quad \frac{dp}{dt} = \partial_x U, \quad x(0) = x_0, \quad p(0) = p_0,$$

then

$$x = X(t, x_0, p_0), \quad p = P(t, x_0, p_0),$$

thus

$$\frac{d}{dt} S(t, x, p, \mathbf{z}) = 2E(X(t, x_0, p_0)),$$

and the analytic solution is given by

$$\begin{aligned} S(t, x, p, \mathbf{z}) &= S_{\text{in}}(x_0, p_0, \mathbf{z}) + 2 \int_0^t E(X(\mu, x_0, p_0, \mathbf{z})) \, d\mu \\ &= 2 \int_0^t E(X(\mu, x_0, p_0, \mathbf{z})) \, d\mu. \end{aligned}$$

Therefore S is an increasing function of t for each (x, p, \mathbf{z}) , since $E > 0$.

The time discretization of W_1, W_2, W_3, W_4 was defined in Section 2.5.2. Denote $\mathcal{E}^\pm(t, x, p, \mathbf{z}) = \tilde{\mathcal{E}}^\pm(S(t, x, p, \mathbf{z}), x, p, \mathbf{z})$. To find the values of \mathcal{E}^\pm at s_l , namely

$$\tilde{\mathcal{E}}^\pm(s_l, x, p, \mathbf{z}) = \mathcal{E}^\pm(t^*, x, p, \mathbf{z}),$$

where $t^* = S^{-1}(s_l)$, for each x_j, p_k , and quadrature points $\mathbf{z}^{(q)}, q = 1, \dots, N_s$, we apply an interpolation step shown here.

Search for the time interval $[t_{n_k}, t_{n_{k+1}}]$ such that s_l falls between the interval $[S(t_{n_k}), S(t_{n_{k+1}})]$, thus $t^* \in [t_{n_k}, t_{n_{k+1}}]$, since S is an increasing function of t . Linear interpolation is used to find t^* . Denote $t_{n_k} = t^{(1)}, t_{n_{k+1}} = t^{(2)}$, and $S(t_{n_k}) = S^{(1)}, S(t_{n_{k+1}}) = S^{(2)}$. By the Lagrange interpolation,

$$s_l = S^{(1)} \frac{t^* - t^{(2)}}{t^{(1)} - t^{(2)}} + S^{(2)} \frac{t^* - t^{(1)}}{t^{(2)} - t^{(1)}},$$

which gives t_* . The values \mathcal{E}^\pm at all t_n have been obtained, one can use linear interpolation to approximate the value of \mathcal{E}^\pm at t^* , for each $x_j, p_k, \mathbf{z}^{(q)}$.

Using the Gauss quadrature rule with quadrature points $\mathbf{z}^{(q)}$ and the corresponding weights $\omega_q, q = 1, \dots, N_g$, we update the matrices $\mathcal{J}, \mathcal{L}, \mathcal{C}$ at each (s_l, x_j, p_k) , and \mathcal{H} at each x_j ,

$$\begin{aligned} \mathcal{J}_{mn}(s_l, x_j, p_k) &= \sum_{q=1}^{N_g} \frac{1}{\tilde{\mathcal{E}}^+(s_l, x_j, p_k, \mathbf{z}^{(q)})} \psi_m(\mathbf{z}^{(q)}) \psi_n(\mathbf{z}^{(q)}) \omega_q, \\ \mathcal{L}_{mn}(s_l, x_j, p_k) &= \sum_{q=1}^{N_g} \frac{1}{\tilde{\mathcal{E}}^-(s_l, x_j, p_k, \mathbf{z}^{(q)})} \psi_m(\mathbf{z}^{(q)}) \psi_n(\mathbf{z}^{(q)}) \omega_q, \\ \mathcal{C}_{mn}(s_l, x_j, p_k) &= \sum_{q=1}^{N_g} \frac{\partial_x E(x_j, \mathbf{z}^{(q)})}{\tilde{\mathcal{E}}^+(s_l, x_j, p_k, \mathbf{z}^{(q)})} \psi_m(\mathbf{z}^{(q)}) \psi_n(\mathbf{z}^{(q)}) \omega_q, \\ \mathcal{H}_{mn}(x_j) &= \sum_{q=1}^{N_g} \frac{1}{2E(x_j, \mathbf{z}^{(q)})} \psi_m(\mathbf{z}^{(q)}) \psi_n(\mathbf{z}^{(q)}) \omega_q. \end{aligned}$$

Step 1. We solve the transport part in x for quantities $\vec{W}_1, \vec{W}_2, \vec{W}_3, \vec{W}_4$ in (3.20),

$$\begin{aligned} \partial_s \vec{W}_1 + p\mathcal{J} \partial_x \vec{W}_1 &= 0, & \partial_s \vec{W}_2 + p\mathcal{J} \partial_x \vec{W}_2 &= 0, \\ \partial_s \vec{W}_3 + p\mathcal{H} \partial_x \vec{W}_3 &= 0, & \partial_s \vec{W}_4 + p\mathcal{H} \partial_x \vec{W}_4 &= 0. \end{aligned}$$

This transport step is treated similarly as in Section 2.2, where we use a pseudo-spectral method in space and a three-stage Runge–Kutta method in time.

Step 2. We solve the transport part in p for W_1, W_2 ,

$$\partial_s \vec{W}_1 - \mathcal{C} \partial_p \vec{W}_1 = 0, \quad \partial_s \vec{W}_2 + \mathcal{C} \partial_p \vec{W}_2 = 0.$$

Similar procedure is taken as in the previous step.

Step 3. We now solve the non-singular source part

$$\begin{aligned} \partial_s \vec{W}_1 &= 2b^i \mathcal{J} \left(\vec{W}_3 \cos \tau + \vec{W}_4 \sin \tau \right), \\ \partial_s \vec{W}_2 &= -2b^i \mathcal{L} \left(\vec{W}_3 \cos \tau + \vec{W}_4 \sin \tau \right), \\ \partial_s \vec{W}_3 &= b^i \mathcal{H} \left(\vec{W}_2 - \vec{W}_1 \right) \cos \tau, \\ \partial_s \vec{W}_4 &= b^i \mathcal{H} \left(\vec{W}_2 - \vec{W}_1 \right) \sin \tau. \end{aligned}$$

We use the forward Euler method,

$$\begin{aligned} \vec{W}_1^{n+1} &= \vec{W}_1^n + 2b^i \Delta s \mathcal{J} \left(\vec{W}_3^n \cos \tau + \vec{W}_4^n \sin \tau \right), \\ \vec{W}_2^{n+1} &= \vec{W}_2^n - 2b^i \Delta s \mathcal{L} \left(\vec{W}_3^n \cos \tau + \vec{W}_4^n \sin \tau \right), \\ \vec{W}_3^{n+1} &= \vec{W}_3^n + b^i \Delta s \mathcal{H} \left(\vec{W}_2^n - \vec{W}_1^n \right) \cos \tau, \\ \vec{W}_4^{n+1} &= \vec{W}_4^n + b^i \Delta s \mathcal{H} \left(\vec{W}_2^n - \vec{W}_1^n \right) \sin \tau. \end{aligned}$$

Other Runge–Kutta methods can also be used to solve this ODE system.

Step 4. Finally, we solve the highly oscillatory part

$$\begin{aligned} \partial_s \vec{W}_1 &= -\frac{1}{\varepsilon} \partial_\tau \vec{W}_1, & \partial_s \vec{W}_2 &= -\frac{1}{\varepsilon} \partial_\tau \vec{W}_2, \\ \partial_s \vec{W}_3 &= -\frac{1}{\varepsilon} \partial_\tau \vec{W}_3, & \partial_s \vec{W}_4 &= -\frac{1}{\varepsilon} \partial_\tau \vec{W}_4. \end{aligned}$$

We use the Fourier transform $\hat{W}_1(\zeta)$ of $W_1(\tau)$ in the τ variable where ζ is the corresponding Fourier variable, then

$$\partial_s \hat{W}_1 = -\frac{i\zeta}{\varepsilon} \hat{W}_1,$$

which is solved by the backward Euler method in time,

$$\hat{W}_1^{n+1}(x_j, p_k) = \left(I + \frac{i\zeta \Delta s}{\varepsilon} I \right)^{-1} \hat{W}_1^n(x_j, p_k).$$

The same method is used for calculating $\vec{W}_2, \vec{W}_3, \vec{W}_4$.

4. NUMERICAL EXAMPLES FOR THE SURFACE HOPPING MODEL

Example 4.1. Consider $x, p \in [-2\pi, 2\pi]$. We use the similar data given in the numerical example in [8], with the following initial conditions,

$$\begin{aligned} f^+(t=0, x, p) &= f^-(t=0, x, p) = (1 + 0.5 \cos(x)) \frac{e^{-p^2/2}}{\sqrt{2\pi}}, \\ f^i(t=0, x, p) &= [1 + 0.5 \sin(x) + i(1 + 0.5 \cos(x))] \frac{e^{-p^2/2}}{\sqrt{2\pi}}. \end{aligned}$$

The expressions for $E, b_i,$ and b^\pm are given by

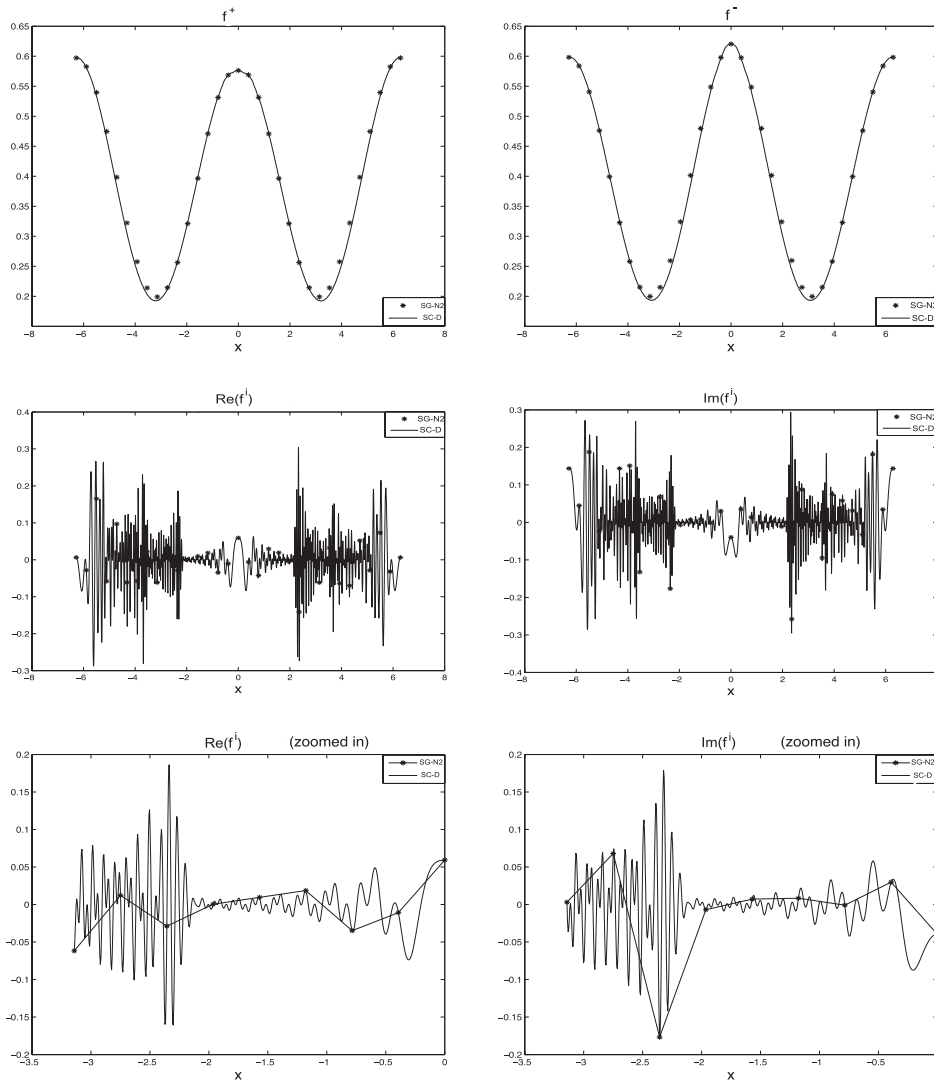


FIGURE 9. Example 4.1. $\varepsilon = 5 \times 10^{-3}$, $t = 0.5$, $N_x = 2500$, $\Delta t = 5 \times 10^{-3}$ (gPC-SC-D), and $N_x = 32$, $\Delta t = 5 \times 10^{-5}$ (gPC-SG-N2). Mean of the space dependence of f^\pm , $\text{Re}(f^i)$ and $\text{Im}(f^i)$ (and their zoomed in solutions) at $p = 0$. Stars: gPC-SG-N2 with $K = 4$. Solid lines: reference solution by gPC-SC-D.

$$E(x, \mathbf{z}) = (1 - \cos(x/2) + \sqrt{\varepsilon})(1 + 0.5\mathbf{z}), \quad b_i(x, p) = -\frac{1}{2} \sin(p + 1), \quad b^\pm = 0.$$

Periodic boundary conditions are considered in x while the p domain is chosen large enough so $f^{\pm,i}$ all vanish outside the domain (thus a periodic boundary condition in p can be used). Without loss of generality we set $U = 0$. For all the following tests, we choose $N_\tau = 8$, $N_p = 32$ and $N_c = 32$ quadrature points for gPC-SC methods (with a very small mesh size in x so this solution is used as the reference solutions).

In Figures 9–11, for gPC-SG-N2 scheme, even if the mesh size is much larger than the wave length $\varepsilon = 5 \times 10^{-3}$, the solution $f^{\pm,i}$ (the mean and standard deviation), as well as $\rho^{\pm,i}$, still agrees with the reference solution at the grid points, despite a moderate gPC order $K = 4$.

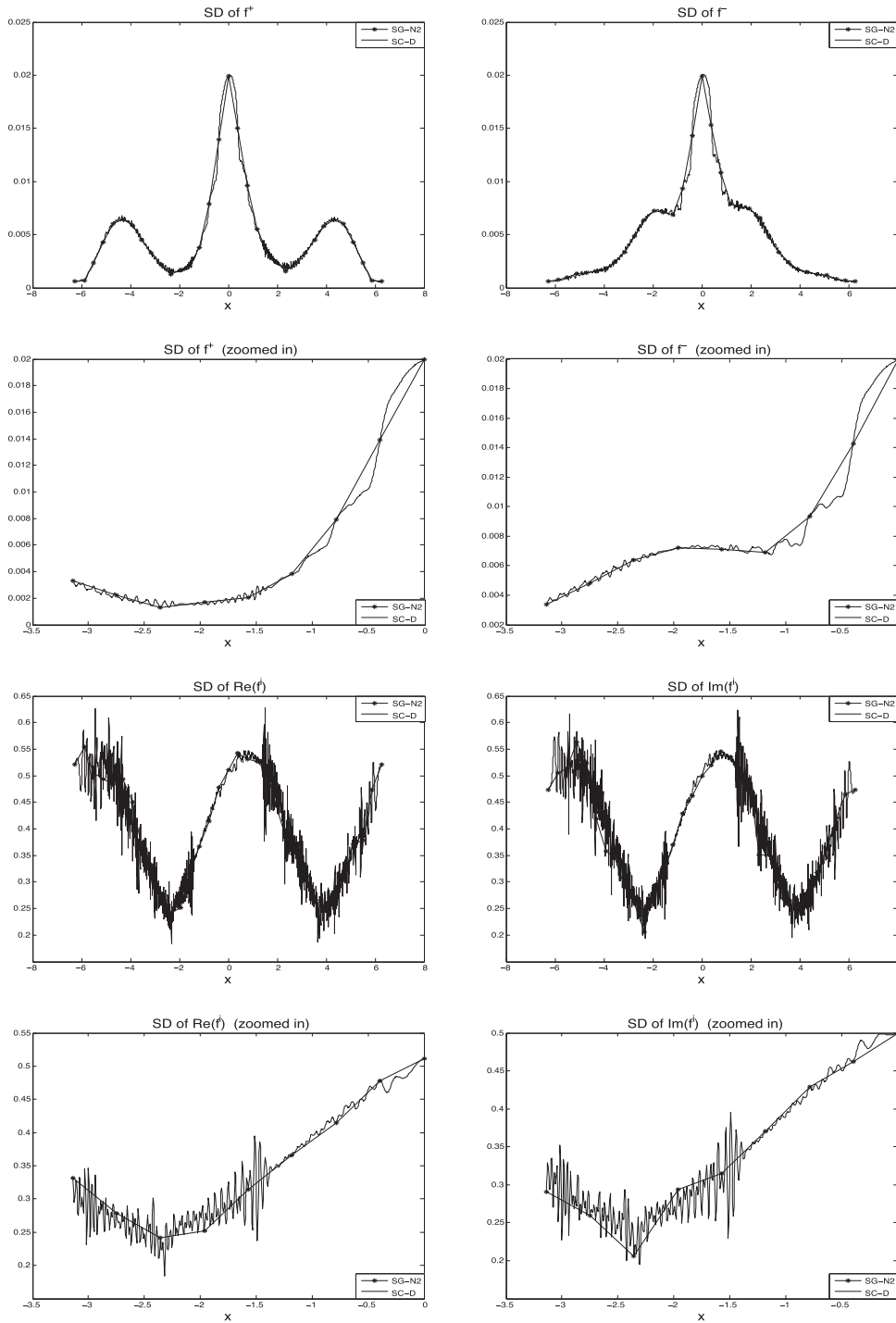


FIGURE 10. Standard deviation of the space dependence of f^\pm , $\text{Re}(f^i)$ and $\text{Im}(f^i)$ (and their zoomed in solutions) at $p = 0$.

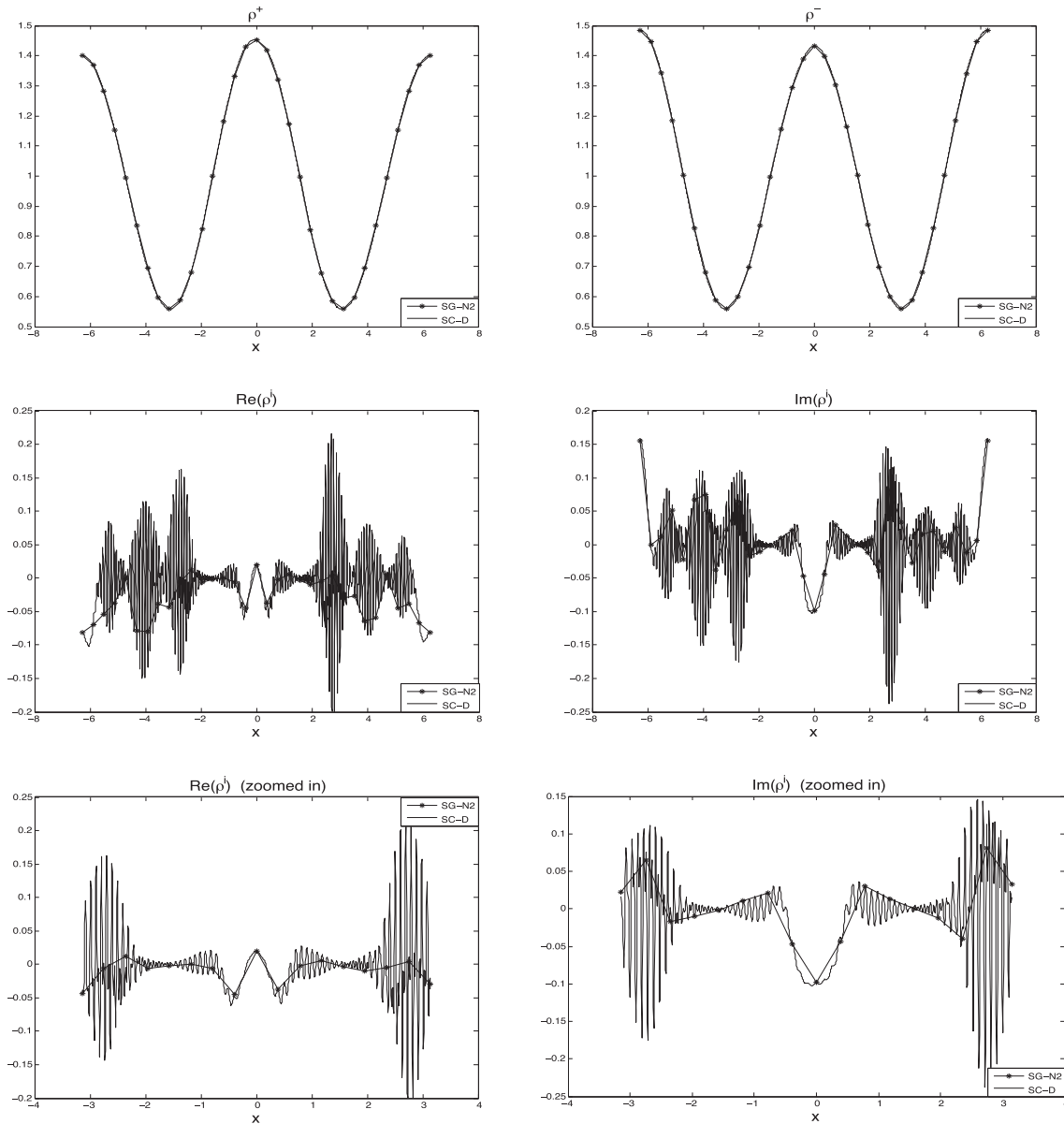


FIGURE 11. Mean of the space dependence of the densities ρ^\pm , $\text{Re}(\rho^i)$ and $\text{Im}(\rho^i)$ (and their zoomed in solutions).

Figure 12 shows a similar result as in Figures 9–11, using Example 4.1 except that here $E(x, \mathbf{z}) = \mathcal{O}(1)$. As discussed in Remark 2.2, small $\Delta t = \mathcal{O}(\sqrt{\varepsilon}\Delta x)$ needs to be chosen in Figures 9–11 due to the CFL condition in the transport steps for $E = \mathcal{O}(\sqrt{\varepsilon})$. However, larger $\Delta t = \mathcal{O}(\Delta x)$, which is independent of ε , can be used in Figure 12 since now $E(x, \mathbf{z}) = \mathcal{O}(1)$.

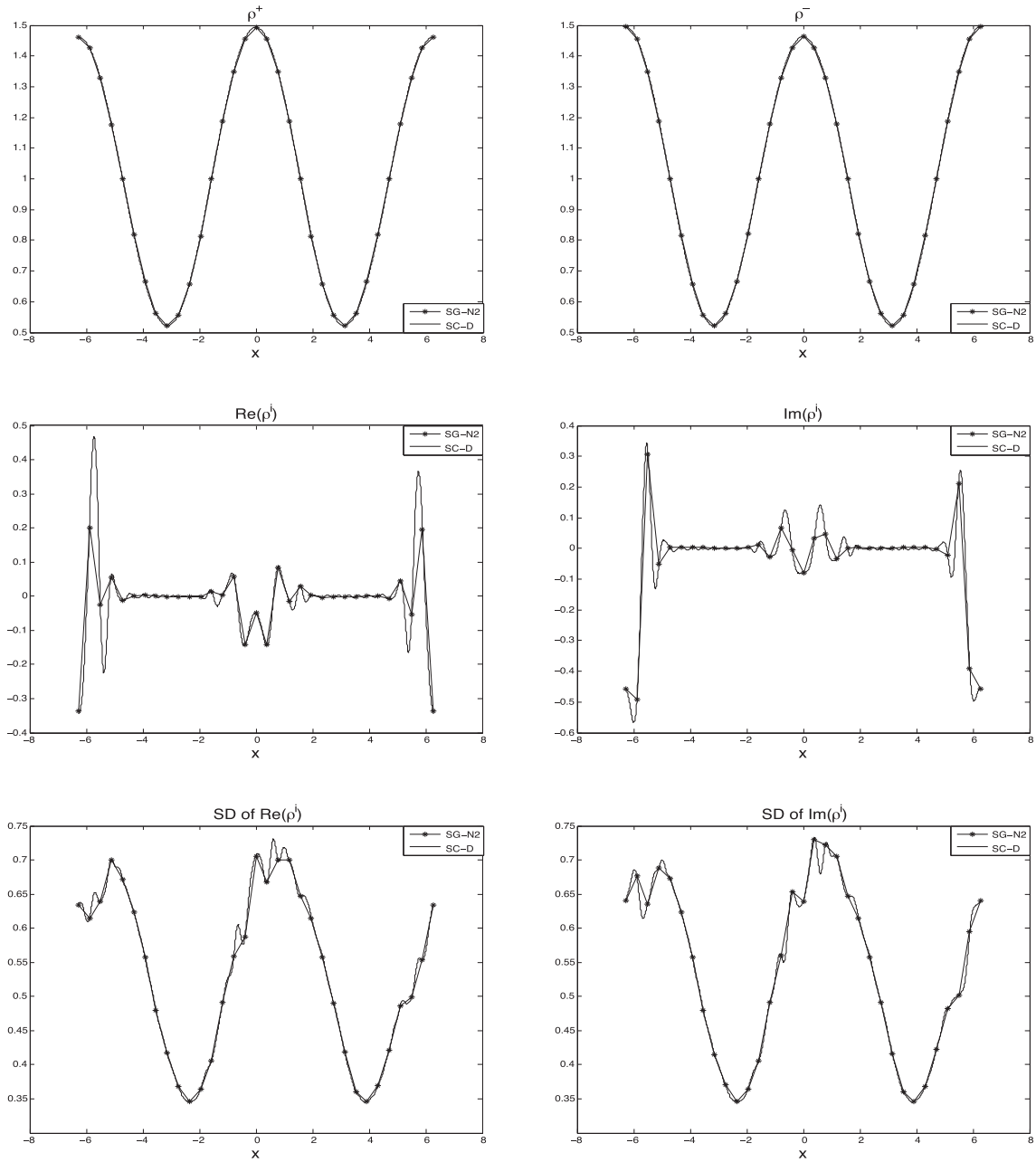


FIGURE 12. Example 4.1, with $E(x, \mathbf{z}) = (10 - \cos(x/2))(1 + 0.5\mathbf{z})$. $\varepsilon = 0.01$, $t = 0.3$, $N_x = 2000$, $\Delta t = 5 \times 10^{-3}$ (gPC-SC-D), and $N_x = 32$, $\Delta t = 0.02$ (gPC-SG-N2). Mean and standard deviation of the space dependence of the densities ρ^\pm , $\text{Re}(\rho^i)$ and $\text{Im}(\rho^i)$. Stars: gPC-SG-N2 with $K = 4$. Solid lines: reference solution by gPC-SC-D.

5. CONCLUSIONS

In this paper, based on a nonlinear geometric optics (NGO) based numerical method developed in [8], with a new “time” variable defined from the phase, we obtain a stochastic Galerkin (SG) method for highly oscillatory transport equations that arise in semiclassical models of non-adiabatic quantum dynamics, in which the potential energy surfaces are assumed to be random, due to uncertainties in modeling or measurement errors. We prove that the generalized polynomial chaos (gPC) based SG method applied directly to the models will require the order of gPC to depend on the possibly very small wave length, while the new method does not have such a requirement. This important property allows us to use this method to solve these highly oscillatory problems with uncertain coefficients with all numerical parameters independent of the wave length, yet still capture the solution statistics pointwisely.

There are several projects along this direction. First it will be desirable to develop an implicit scheme for the transport steps in order to obtain an improved time step constraint when the bad gap becomes very small. Second, methods for higher dimensional–in space, velocity as well as the random variables–remain to be developed.

APPENDIX A. THE gPC-SG-N1 AND gPC-SG-D FOR THE SURFACE HOPPING MODEL WITH RANDOM INPUTS

A.1. The gPC approximation

In this part, we detail the gPC-SG-N1 strategy for model (3.1), based on the method developed in [8] for the deterministic problem. Solving for S follows the same strategy presented in Section 3.2.2 on the gPC-SG-N2 method.

Now we focus on the approximation of the profiles (F^+, F^-, G, H) . One inserts the Galerkin approximation of each component

$$(F^+, F^-, G, H)(t, x, p, \mathbf{z}) = \sum_{j=1}^K (F_j^+, F_j^-, G_j, H_j)(t, x, p) \tilde{\psi}_j(\mathbf{z}),$$

into (3.11) and conduct the gPC Galerkin projection. Denote the associated gPC coefficients vector of $(\vec{F}^+, \vec{F}^-, \vec{G}, \vec{H})$ as previously, for instance for \vec{F}^+ ,

$$\vec{F}^+ = (F_1^+, \dots, F_K^+)^T. \tag{A.1}$$

Then, we get the gPC system

$$\begin{cases} \partial_t \vec{F}^+ + p \partial_x \vec{F}^+ - \mathcal{C} \partial_p \vec{F}^+ = \frac{1}{\varepsilon} (-2\mathcal{C} + \mathcal{H}) \partial_\tau \vec{F}^+ + 2b^i (\vec{G} \cos \tau + \vec{H} \sin \tau), \\ \partial_t \vec{F}^- + p \partial_x \vec{F}^- + \mathcal{C} \partial_p \vec{F}^- = \frac{1}{\varepsilon} (-2\mathcal{C} - \mathcal{H}) \partial_\tau \vec{F}^- - 2b^i (\vec{G} \cos \tau + \vec{H} \sin \tau), \\ \partial_t \vec{G} + p \partial_x \vec{G} = -\frac{2\mathcal{C}}{\varepsilon} \partial_\tau \vec{G} - b^i \vec{F}^+ \cos \tau + b^i \vec{F}^- \cos \tau, \\ \partial_t \vec{H} + p \partial_x \vec{H} = -\frac{2\mathcal{C}}{\varepsilon} \partial_\tau \vec{H} - b^i \vec{F}^+ \sin \tau + b^i \vec{F}^- \sin \tau, \end{cases} \tag{A.2}$$

where matrices $\mathcal{C} \in \mathbb{R}_{K \times K}$ and $\mathcal{H} \in \mathbb{R}_{K \times K}$ are defined by

$$\begin{aligned} \mathcal{C}_{mn}(x) &= \int_{I_{\mathbf{z}}} E(x, \mathbf{z}) \tilde{\psi}_m(\mathbf{z}) \tilde{\psi}_n(\mathbf{z}) \, d\mathbf{z}, \quad 1 \leq m, n \leq K, \\ \mathcal{H}_{km}(t, x, p) &= \sum_{l=1}^K \partial_p \tilde{S}_l(t, x, p) D_{lmk}(x), \quad 1 \leq k, m \leq K, \end{aligned}$$

with $\partial_p \tilde{S}_l(t, x, p)$ ($l = 1, \dots, K$) the gPC coefficients of $\partial_p S(t, x, p, \mathbf{z})$, *i.e.*,

$$\partial_p \vec{S}(t, x, p) = \left(\partial_p \tilde{S}_1(t, x, p), \dots, \partial_p \tilde{S}_K(t, x, p) \right)^T,$$

and the tensor $D(x)$ is given by

$$D_{lmk}(x) = \int_{I_{\mathbf{z}}} \partial_x E(x, \mathbf{z}) \tilde{\psi}_l(\mathbf{z}) \tilde{\psi}_m(\mathbf{z}) \tilde{\psi}_k(\mathbf{z}) \pi(\mathbf{z}) \, d\mathbf{z}.$$

Note that the matrix \mathcal{H} is symmetric.

The initial conditions have been discussed in Section 3.2.2.

A.2. The fully discrete scheme gPC-SG-N1

To solve (A.2), we use a time splitting procedure. We split the equation into four steps: two transport steps (in x and in p), a highly oscillatory part and a non-singular source part. We detail how we solve each step in the sequel.

Step 1. We solve the transport part in x for each quantity F^+, F^-, G, H . For example, to solve the transport in F^+ ,

$$\partial_t \vec{F}^+ + p \partial_x \vec{F}^+ = 0,$$

we use a spectral method in space and an exact integration in time in the Fourier space, that is

$$\vec{F}^{+,n+1}(\xi) = e^{-ip\xi\Delta t} \vec{F}^{+,n}(\xi), \tag{A.3}$$

where ξ denotes the Fourier space variable and $\hat{F}^+(\xi)$ the corresponding (discrete) Fourier transform. Finally, $\vec{F}^{+,n+1}$ is obtained by the inverse Fourier transform.

Step 2. We solve the transport part in p for F^\pm ,

$$\partial_t \vec{F}^\pm \mp \mathcal{C} \partial_p \vec{F}^\pm = 0.$$

We also use a spectral method in p and an exact integration in time in the Fourier space, that is

$$\vec{F}^{\pm,n+1}(\eta) = e^{\pm i\eta \mathcal{C}(x) \Delta t} \vec{F}^{\pm,n}(\eta), \tag{A.4}$$

where η is the Fourier velocity variable. Finally $\vec{F}^{\pm,n+1}$ are obtained by the inverse Fourier transform.

Step 3. We now solve the non-singular source part

$$\partial_t \vec{F}^+ = 2b^i \left(\vec{G} \cos \tau + \vec{H} \sin \tau \right), \tag{A.5}$$

$$\partial_t \vec{F}^- = -2b^i \left(\vec{G} \cos \tau + \vec{H} \sin \tau \right), \tag{A.6}$$

$$\partial_t \vec{G} = -b^i \vec{F}^+ \cos \tau + b^i \vec{F}^- \cos \tau, \tag{A.7}$$

$$\partial_t \vec{H} = -b^i \vec{F}^+ \sin \tau + b^i \vec{F}^- \sin \tau. \tag{A.8}$$

This linear system with time independent coefficients can be solved exactly.

Step 4. Finally, we solve the highly oscillatory part

$$\partial_t \vec{F}^+ = \frac{1}{\varepsilon} (-2\mathcal{C} + \mathcal{H}) \partial_\tau \vec{F}^+, \quad \partial_t \vec{F}^- = \frac{1}{\varepsilon} (-2\mathcal{C} - \mathcal{H}) \partial_\tau \vec{F}^-,$$

$$\partial_t \vec{G} = -\frac{2\mathcal{C}}{\varepsilon} \partial_\tau \vec{G}, \quad \partial_t \vec{H} = -\frac{2\mathcal{C}}{\varepsilon} \partial_\tau \vec{H}.$$

We use the Fourier transform $\hat{F}(\zeta)$ of $F(\tau)$ in the τ variable where ζ is the corresponding Fourier variable. Then, we have

$$\begin{aligned}\partial_t \vec{F}^+ &= \frac{i\zeta}{\varepsilon}(-2\mathcal{C} + \mathcal{H})\vec{F}^+, & \partial_t \vec{F}^- &= \frac{i\zeta}{\varepsilon}(-2\mathcal{C} - \mathcal{H})\vec{F}^-, \\ \partial_t \vec{G} &= \frac{i\zeta}{\varepsilon}(-2\mathcal{C})\vec{G}, & \partial_t \vec{H} &= \frac{i\zeta}{\varepsilon}(-2\mathcal{C})\vec{H},\end{aligned}$$

which is solved by the backward Euler method in time,

$$\vec{F}^{+,n+1} = \left[I - \frac{i\zeta}{\varepsilon} \Delta t (-2\mathcal{C} + \mathcal{H}) \right]^{-1} \vec{F}^{+,n}, \quad (\text{A.9})$$

$$\vec{F}^{-,n+1} = \left[I - \frac{i\zeta}{\varepsilon} \Delta t (-2\mathcal{C} - \mathcal{H}) \right]^{-1} \vec{F}^{-,n}, \quad (\text{A.10})$$

$$\vec{G}^{n+1} = \left[I + 2\frac{i\zeta}{\varepsilon} \Delta t \mathcal{C} \right]^{-1} \vec{G}^n, \quad (\text{A.11})$$

$$\vec{H}^{n+1} = \left[I + 2\frac{i\zeta}{\varepsilon} \Delta t \mathcal{C} \right]^{-1} \vec{H}^n. \quad (\text{A.12})$$

Notice that we have already solved the gPC coefficients vector $\vec{S}(t, x, p)$ from (3.17). This allows to compute $\partial_p \vec{S}(t, x, p)$ spectrally (using Fourier in p) which is used in the expression of matrix $\left(I - \frac{i\zeta}{\varepsilon} \Delta t (-2\mathcal{C} \pm \mathcal{H}) \right)$.

Note that the matrices in (A.9)–(A.12) are invertible since they are symmetric and have real eigenvalues.

A.3. The gPC-SG-D scheme

We briefly introduce the gPC-SG-D for the surface hopping model with random inputs. One first inserts the gPC expansions

$$(f^+, f^-, g, h)(t_n, x, p, \mathbf{z}) \approx \sum_{j=1}^K \left(\tilde{f}_j^{+,n}, \tilde{f}_j^{-,n}, \tilde{g}_j^n, \tilde{h}_j^n \right) (x, p) \tilde{\psi}_j(\mathbf{z}),$$

into equation (3.8). Then, denoting as previously $\vec{g}^n = (\tilde{g}_1^n, \tilde{g}_2^n, \dots, \tilde{g}_K^n)$ (and the same notations for $\vec{f}^{+,n}, \vec{f}^{-,n}, \vec{h}^n$), we conduct the Galerkin projection to get

$$\begin{aligned}\vec{g}^{n+1} &= \left[I + (b^i)^2 (\Delta t)^2 I + \frac{\Delta t^2}{\varepsilon^2} \mathcal{P} \right]^{-1} \\ &\times \left[\vec{g}^n + \Delta t \left(-b^i \vec{f}^{+,n} + b^i \vec{f}^{-,n} + \frac{2}{\varepsilon} \mathcal{W} \vec{h}^n - (b^i)^2 \Delta t \vec{g}^n - \frac{\Delta t}{\varepsilon^2} \mathcal{P} \vec{g}^n \right) \right],\end{aligned}$$

where the matrices $\mathcal{W}_{K \times K}$ and $\mathcal{P}_{K \times K}$ are defined by

$$\mathcal{W}(x)_{ml} = \int_{I_{\mathbf{z}}} E(x, \mathbf{z}) \psi_m(\mathbf{z}) \psi_l(\mathbf{z}) \pi(\mathbf{z}) d\mathbf{z}, \quad 1 \leq m, l \leq K,$$

$$\mathcal{P}(x)_{ml} = \int_{I_{\mathbf{z}}} E(x, \mathbf{z})^2 \psi_m(\mathbf{z}) \psi_l(\mathbf{z}) \pi(\mathbf{z}) d\mathbf{z}, \quad 1 \leq m, l \leq K.$$

Since \mathcal{P} is symmetric and positive definite, with positive eigenvalues, so does the matrix $\left(I + (b^i)^2 (\Delta t)^2 I + \frac{\Delta t^2}{\varepsilon^2} \mathcal{P} \right)$, thus it is invertible. Since \vec{g}^{n+1} is known, we can compute $\vec{f}^{+,n+1}, \vec{f}^{-,n+1}$,

\vec{h}^{n+1} by gPC approximation of (3.4), (3.5) and (3.7) as

$$\begin{aligned}\vec{f}^{+,n+1} &= \vec{f}^{+,n} + b^i \Delta t (\vec{g}^n + \vec{g}^{n+1}), \\ \vec{f}^{-,n+1} &= \vec{f}^{-,n} - b^i \Delta t (\vec{g}^n + \vec{g}^{n+1}), \\ \vec{h}^{n+1} &= \vec{h}^n - \frac{\Delta t}{\varepsilon} \mathcal{W}(\vec{g}^n + \vec{g}^{n+1}).\end{aligned}$$

Acknowledgements. This work has been supported by the EURO fusion Consortium and has received funding from the Euratom research and training programme 2019–2020 under grant agreement no. 633053. S. Jin is supported by NSFC grants no. 11871297 and no. 31571071.

REFERENCES

- [1] M. Born and R. Oppenheimer, Zur quantentheorie der molekeln [on the quantum theory of molecules]. *Ann. Phys.* **389** (1927) 457–484.
- [2] A. Castro Neto, F. Guinea, N. Peres, K. Novoselov and A. Geim, The electronic properties of graphene. *Phys. Mod. Phys.* **81** (2009) 109–162.
- [3] L. Chai, S. Jin and Q. Li, Semi-classical models for the Schrödinger equation with periodic potentials and band crossings. *Kinet. Relat. Models* **6** (2013) 505–532.
- [4] L. Chai, S. Jin, Q. Li and O. Morandi, A multiband semiclassical model for surface hopping quantum dynamics. *Multiscale Model. Simul.* **13** (2015) 205–230.
- [5] P. Chartier, N. Crouseilles, M. Lemou and F. Méhats, Uniformly accurate numerical schemes for highly-oscillatory Klein–Gordon and nonlinear Schrödinger equations. *Numer. Math.* **129** (2015) 211–250.
- [6] H. Choi and J. Liu, The reconstruction of upwind fluxes for conservation laws: its behavior in dynamic and steady state calculations. *J. Comput. Phys.* **144** (1998) 237–256.
- [7] N. Crouseilles, M. Lemou and F. Méhats, Asymptotic preserving schemes for highly-oscillatory Vlasov–Poisson equations. *J. Comput. Phys.* **248** (2013) 287–308.
- [8] N. Crouseilles, S. Jin and M. Lemou, Nonlinear geometric optics method based multi-scale numerical schemes for highly-oscillatory transport equations. *Math. Models Methods Appl. Sci.* **23** (2017) 2031–2070.
- [9] B. Engquist and O. Runborg, Computational high frequency wave propagation. *Acta Numer.* **12** (2003) 181–266.
- [10] C.L. Fefferman and M.I. Weinstein, Honeycomb lattice potentials and Dirac points. *J. Am. Math. Soc.* **25** (2012) 1169–1220.
- [11] R.G. Ghanem and P.D. Spanos, Stochastic Finite Elements: A Spectral Approach. Springer-Verlag, New York (1991).
- [12] D. Gottlieb and D. Xiu, Galerkin method for wave equations with uncertain coefficients. *Commun. Comput. Phys.* **3** (2008) 505–518.
- [13] M.D. Gunzburger, C.G. Webster and G. Zhang, Stochastic finite element methods for partial differential equations with random input data. *Acta Numer.* **23** (2014) 521–650.
- [14] O.P. Le Maître and O.M. Knio, Spectral Methods for Uncertainty Quantification, with Applications to Computational Fluid Dynamics. Scientific Computation. Springer, New York (2010).
- [15] O. Morandi, Effective classical Liouville-like evolution equation for the quantum phase-space dynamics. *J. Phys. A* **43** (2010) 365302.
- [16] O. Morandi and F. Schürer, Wigner model for Klein tunneling in graphene. *J. Phys. A* **44** (2011) 265301.
- [17] R.G. Parr, Density Functional Theory of Atoms and Molecules. Horizons of Quantum Chemistry. Springer (1980) 5–15.
- [18] J. Proppe, T. Husch, G.N. Simm and M. Reiher, Uncertainty quantification for quantum chemical models of complex reaction networks. *Faraday Discuss.* **195** (2017) 497–520.
- [19] B. Ruscic, Uncertainty quantification in thermochemistry, benchmarking electronic structure computations, and active thermochemical tables. *Int. J. Quantum Chem.* **114** (2014) 1097–1101.
- [20] J. Shen, T. Tang and L.-L. Wang, Spectral Methods: Algorithms, Analysis and Applications. Springer, Heidelberg **41** (2011).
- [21] J. Tully, Molecular dynamics with electronic transitions. *J. Chem. Phys.* **93** (1990) 1061–1071.
- [22] J. Tully and R. Preston, Trajectory surface hopping approach to nonadiabatic molecular collisions: the reaction of h^+ with d_2 . *J. Chem. Phys.* **55** (1971) 562–572.
- [23] T. van Mourik and R.J. Gdanitz, A critical note on density functional theory studies on rare-gas dimers. *J. Chem. Phys.* **116** (2002) 9620–9623.
- [24] J. Vondrasek, L. Bendova, V. Klusak and P. Hobza, Unexpectedly strong energy stabilization inside the hydrophobic core of small protein rubredoxin mediated by aromatic residues: correlated ab initio quantum chemical calculations. *J. Am. Chem. Soc.* **127** (2005) 2615–2619.

- [25] B. Wu and Q. Niu, Nonlinear Landau-Zener tunneling. *Phys. Rev. A.* **61** (2000) 023402.
- [26] D. Xiu, Numerical Methods for Stochastic Computations: A Spectral Method Approach. Princeton University Press, Princeton, NJ, USA (2010).
- [27] D. Xiu and J.S. Hesthaven, High-order collocation methods for differential equations with random inputs. *SIAM J. Sci. Comput.* **27** (2005) 1118–1139.
- [28] D. Xiu and G.E. Karniadakis, The Wiener–Askey polynomial chaos for stochastic differential equations. *SIAM J. Sci. Comput.* **24** (2002) 619–644.